研究分担者　岡　慎一

1. Nishijima T, Takano M, Ishisaka M, Komastu H, Gatanaga H, Kikuchi Y, Endo T, Horiba M, Kaneda S, Uchiumi H, Koibuchi T, Naito T, Yoshida M, Tachikawa N, Ueda M, Yokomaku Y, Fujii T, Higasa S, Takada K, Yamamoto M, Matsushita S, Tateyama M, Tanabe Y, Mistuya H, and Oka S on behalf of the Epzicom-Truvada study team. Abacavir/Lamivudine versus Tenofovir/Emtricitabine with Atazanavir/ Ritonavir for treatment naïve HIV-infected Japanese: a randomized multisite trial. Intern Med 52;735-744, 2013.
2. Gatanaga H, Hayashida T, Tanuma J, and Oka S. Prophylactic effect of antiretroviral therapy on Hepatitis B Virus infection. Clin Infect Dis 56 (12); 1812-1819, 2013.
3. Hamada Y, Nagata N, Shimbo T, Igari T, Nakashima R, Asayama N, Nishimura S, Yazaki H, Teruya K, Gatanaga H, Kikuchi Y, Akiyama J, Ohmagari N, Uemura N and Oka S. Assessment of antigenemia assay for the diagnosis of cytomegalovirus gastrointestinal diseases in HIV-infected patients. AIDS Patient Care STD 27 (7) ; 387-391, 2013.
4. Tanuma J, Sano K, Teruya K, Watanabe K, Aoki T, Honda H, Yazaki H, Tsukada K, Gatanaga H, Kikuchi Y, and Oka S. Pharmacokinetics of rifabutin in Japanese HIV-infected patients with or without antiretroviral therapy. PLOS One 8 (8); e70611, 2013.
5. Mizushima D, Nishijima T, Gatanaga H, Tsukada K, Teruya K, Kikuchi Y, Oka S. Preemptive therapy prevents cytomegalovirus end-organ disease in treatment-naïve patients with advanced HIV-1 Infection in the HAART era. PLOS One 8 (5); e65348, 2013.
6. Tsuchiya K, Ode H, Hayashida T, Kakizawa J, Sato H, Oka S, and Gatanaga H. Arginine Insertion and Loss of N-linked Glycosylation Site in HIV-1 Envelope V3 Region Confer CXCR4-tropism. Scientific Report 3; 2389, 2013
7. Gatanaga H, Murakoshi H, Hachiya A, Hayashida T, Chikata T, Ode H, Tsuchiya K, Sugiura W, Takiguchi M, and Oka S. Naturally Selected Rilpivirine-Resistant HIV-1 Variants by Host Cellular Immunity. Clin Infect Dis 57 (7); 1051-1055, 2013.
8. Hamada Y, Nishijima T, Komatsu H, Teruya K, Gatanaga H, Kikuchi Y, and Oka S. Is ritonavir-boosted atazanavir a risk for cholelithiasis compared to other protease inhibitors? PLOS One 8 (7); e69845, 2013.
9. Nishijima T, Gatanaga H, Komatsu H, Takano M, Ogane M, Ikeda K, and Oka S. Illicit drug use is a significant risk factor for loss to follow up in patients with HIV-1 infection at a large urban HIV clinic in Tokyo. PLOS One 8 (8); e72310, 2013.
10. Nishijima T, Gatanaga H, Shimbo T, Komatsu H, Endo T, Horiba M, Koga M, Naito T, Itoda I, Tei M, Fujii T, Takada K, Yamamoto M, Miyakawa T, Tanabe Y, Mitsuya H, and **Oka S** on behalf of the SPARE study team. Switching tenofovir/emtricitabine plus lopinavir/r to raltegravir plus darunavir/r in patients with suppressed viral load did not result in improvement of renal function but could sustain viral suppression: A randomized multicenter trial. PLOS One 8 (8); e73639, 2013.
11. Watanabe K, Murakoshi H, Tamura Y, Koyanagi M, Chikata T, Gatanaga H, Oka S, and Takiguchi M. Identification of cross-clade CTL epitopes in HIV-1 clade A/E-infected individuals by using the clade B overlapping peptides. Microb Infect 15; 874-886, 2013.
12. Nishijima T, Gatanaga H, Komatsu H, Takano M, Ogane M, Ikeda K, Oka S. High prevalence of illicit drug use in men who have sex with men with HIV-1 infection in Japan. PLOS One 8 (12); e81960, 2013.
13. Mizushima D, Tanuma J, Kanaya F, Nishijima T, Gatanaga H, Lam NT, Dung NTH, Kinh NV, Kikuchi Y and Oka S. WHO antiretroviral therapy guidelines 2010 and impact of tenofovir on chronic kidney disease in Vietnamese HIV-infected patients. PLOS One 8 (11); e79885, 2013.
14. Nishijima T, Hamada Y, Watanabe K, Komatsu H, Kinai E, Tsukada K, Teruya K, Gatanaga H, Kikuchi Y, and Oka S. Ritonavir-boosted darunavir is rarely associated with nephrolithiasis compared with ritonavir-boosted atazanavir in HIV-infected patients. PLOS One 8 (10); e77268, 2013.
15. Nishijima T, Shimbo T, Komastu H, Hamada Y, Gatanaga H, and Oka S. Incidence and risk factors for incident hepatitis C infection among men who have sex with men with HIV-1 infection in a large urban HIV clinic in Tokyo. JAIDS 65 (2); 213-217, 2014.

16. Nishijima T, Gatanaga H, Shimbo T, Komatsu H, Nozaki Y, Nagata N, Kikuchi Y, Yanase M and Oka S. Traditional but not HIV-related factors are associated with nonalcoholic fatty liver disease in Asian patients with HIV-1 infection. PLOS One 9 (1); e87596, 2014.
17. Hamada Y, Nagata N, Nishijima T, Shimbo T, Asayama N, Kishida Y, Sekine K, Tanaka S, Aoki T, Watanabe K, Akiyama J, Igari T, Mizokami M, Uemura N, and Oka S. Impact of HIV Infection on Colorectal Tumors, Prospective Colonoscopic Study of Asia patients. JAIDS 65 (3); 312-317, 2014.
18. Matsunaga A, Hishima T, Tanaka N, Yamasaki M, Yoshida L, Mochizuki M, Tanuma J, Oka S, Ishizaka Y, Shimura M and Hagiwara S. DNA methylation profiling can classify HIV-associated lymphomas. **AIDS** 28(4); 503-510, 2014.
19. Suzuki Y, Gatanaga H, Tachikawa N and Oka S. Slow turnover of HIV-1 receptors on quiescent $CD4^+$ T cells causes prolonged surface retention of gp120 immune complexes *in vivo*. PLOS One 9 (2); e86479, 2014.
20. Watanabe K, Aoki T, Nagata N, Tanuma J, Kikuchi Y, Oka S and Gatanaga H. Clinical significance of high anti-*Entamoeba histolytica* antibody titer in asymptomatic HIV-1-infected individuals. J Infect Dis 2013, Dec 13. [Epub ahead of print]
21. Nishijima T, Shimbo T, Komatsu H, Hamada Y, Gatanaga H, Kikuchi Y and Oka S. Cumulative exposure to ritonavir-boosted atazanavir is associated with cholelithiasis in patients with HIV-1 infection. **J Antimicrob Chemothera** 2013 Dec 29. [Epub ahead of print]
22. Kinai E, Nishijima T, Mizushima D, Watanabe K, Aoki T, Honda H, Yazaki H, Genka I, Tanuma J, Teruya K, Tsukada K, Gatanaga H, Kikuchi Y, and Oka S. Prevalence and risk factors of bone mineral density abnormalities in Japanese HIV-infected patients. AIDS Res Hum Retrovirol (in press)

研究分担者　宮川　寿一

1. Nishijima T, Gatanaga H, Shimbo T, Komatsu H, Ishisaka M, Tsukada K, Endo T, Horiba M, Koga M, Naito T, Itoda I, Tei M, Fujii T, Takada K, Yamamoto M, Miyakawa T, Tanabe Y, Mitsuya H, and Oka S on behalf of the SPARE study team. Switching tenofovir/emtricitabine plus lopinavir/r to raltegravir plus darunavir/r in patients with suppressed viral load does not result in recovery of renal function but could sustain viral suppression: A randomized multicenter trial. PLOS One 8 (8); e73639, 2013.

AAC
Journals.ASM.org

GRL-04810 and GRL-05010, Difluoride-Containing Nonpeptidic HIV-1 Protease Inhibitors (PIs) That Inhibit the Replication of Multi-PI-Resistant HIV-1 *In Vitro* and Possess Favorable Lipophilicity That May Allow Blood-Brain Barrier Penetration

Pedro Miguel Salcedo Gómez,[a] Masayuki Amano,[a] Sofiya Yashchuk,[b] Akira Mizuno,[b] Debananda Das,[c] Arun K. Ghosh,[b] Hiroaki Mitsuya[a,c]

Departments of Infectious Diseases and Hematology, Kumamoto University School of Medicine, Kumamoto, Japan[a]; Departments of Chemistry and Medicinal Chemistry, Purdue University, West Lafayette, Indiana, USA[b]; Experimental Retrovirology Section, HIV and AIDS Malignancy Branch, National Cancer Institute, National Institutes of Health, Bethesda, Maryland, USA[c]

We designed, synthesized, and identified two novel nonpeptidic human immunodeficiency virus type 1 (HIV-1) protease inhibitors (PIs), GRL-04810 and GRL-05010, containing the structure-based designed privileged cyclic ether-derived nonpeptide P2 ligand, *bis*-tetrahydrofuranylurethane (*bis*-THF), and a difluoride moiety, both of which are active against the laboratory strain HIV-1_{LAI} (50% effective concentrations [EC_{50}s], 0.0008 and 0.003 μM, respectively) with minimal cytotoxicity (50% cytotoxic concentrations [CC_{50}s], 17.5 and 37.0 μM, respectively, in $CD4^+$ MT-2 cells). The two compounds were active against multi-PI-resistant clinical HIV-1 variants isolated from patients who had no response to various antiviral regimens. GRL-04810 and GRL-05010 also blocked the infectivity and replication of each of the HIV-1_{NL4-3} variants selected by up to 5 μM lopinavir (EC_{50}s, 0.03 and 0.03 μM, respectively) and atazanavir (EC_{50}s, 0.02 and 0.04 μM, respectively). Moreover, they were active against darunavir (DRV)-resistant variants (EC_{50} in 0.03 to 0.034 μM range for GRL-04810 and 0.026 to 0.043 μM for GRL-05010), while DRV had EC_{50}s between 0.02 and 0.174 μM. GRL-04810 had a favorable lipophilicity profile as determined with the partition (log *P*) and distribution (log *D*) coefficients of −0.14 and −0.29, respectively. The *in vitro* blood-brain barrier (BBB) permeability assay revealed that GRL-04810 and GRL-05010 may have a greater advantage in terms of crossing the BBB than the currently available PIs, with apparent penetration indexes of 47.8×10^{-6} and 61.8×10^{-6} cm/s, respectively. The present data demonstrate that GRL-04810 and GRL-05010 exert efficient activity against a wide spectrum of HIV-1 variants *in vitro* and suggest that two fluorine atoms added to their *bis*-THF moieties may well enhance their penetration across the BBB.

Combined antiretroviral therapy (cART) has had a major impact on the AIDS epidemic; however, no eradication of human immunodeficiency virus type 1 (HIV-1) appears to be readily possible, in part due to the viral reservoirs remaining in blood and infected tissues. Moreover, we have encountered a number of challenges in bringing about the optimal benefits of the currently available therapeutics of HIV-1 infection and AIDS to individuals receiving cART (1–6). These challenges include (i) drug-related toxicities, (ii) partial restoration of immunologic functions once individuals develop AIDS, (iii) development of various cancers as a consequence of survival prolongation, (iv) immune reconstitution syndrome (IRS) or flare-ups of inflammation in individuals receiving cART, and (v) increased cost of antiviral therapy. Such limitations and flaws of cART are exacerbated by the development of drug-resistant HIV-1 variants (7–11).

One of the sanctuary sites for HIV-1 infection is the central nervous system (CNS) (12). The fact that HIV-1 enters and infects target cells in the CNS represents a significant challenge for the long-term suppression of virus replication and has been linked to the development of several neurological complications (13, 14). Although cART has significantly reduced the incidence of HIV-1-associated dementia, the prevalence of CNS disorders such as HIV-1-associated neurocognitive disorders, or HAND, appears to be increasing as a result of prolonged patient survival and poor antiretroviral drug penetration into the CNS (15–19). Furthermore, subtherapeutic drug concentrations in the CNS may facilitate the development of viral resistance (20). In addition, HIV-1 infection of the CNS may also result in the establishment of a unique viral reservoir, which certain antiretroviral drugs do not have reasonable access to (21–24). Moreover, there is evidence that cART is less effective in lowering virus replication in the CNS than in the blood (21), and unfortunately HIV protease inhibitors (PIs) and several of the nucleoside analogs penetrate only poorly into the CNS (12), allowing early CNS infection to evolve independently over time in the inaccessible brain reservoir (25).

Successful antiviral drugs, in theory, exert their virus-specific effects by interacting with viral receptors, virally encoded enzymes, viral structural components, or viral genes or their transcripts without disturbing cellular metabolism or function. However, at present, no antiretroviral drugs or agents are likely to be completely specific for HIV-1 or to be devoid of toxicity in the

Received 4 July 2013 Returned for modification 29 July 2013
Accepted 19 September 2013
Published ahead of print 30 September 2013
Address correspondence to Masayuki Amano, mamano@kumamoto-u.ac.jp.
Supplemental material for this article may be found at http://dx.doi.org/10.1128/AAC.01420-13.

doi:10.1128/AAC.01420-13

therapy of AIDS, which is a critical issue because patients with AIDS and its related diseases will have to receive cART for a long period of time, perhaps for the rest of their lives. Thus, the identification of a new class of antiretroviral drugs which have a unique mechanism(s) of action and produce no or minimal side effects remains an important therapeutic objective.

We have been focusing on the design and synthesis of nonpeptidyl protease inhibitors (PIs) that are capable of overcoming HIV-1 variants resistant to the currently approved PIs. One such anti-HIV-1 agent, darunavir (DRV), containing a structure-based designed privileged nonpeptidic P2 ligand, 3(*R*),3a(*S*),6a(*R*)-*bis*-tetrahydrofuranylurethane (*bis*-THF) (26–28), has been clinically used worldwide as a first-line therapeutic for HIV-1-infected individuals. In the present work, we designed and synthesized nonpeptidic HIV-1 protease inhibitors GRL-04810 and GRL-05010, which contain *bis*-THF and a difluoride moiety, and found that these compounds exert efficacious activity against a wide spectrum of laboratory HIV-1 strains and primary clinical isolates, including multi-PI-resistant variants, with minimal cytotoxicity. We also attempted to elucidate the binding interactions of the two compounds with the wild-type HIV-1 protease by employing molecular modeling. Moreover, we selected HIV-1 variants with GRL-04810 and GRL-05010 by propagating a laboratory wild-type HIV-1_{NL4-3} in MT-4 cells in the presence of increasing concentrations of GRL-04810 and GRL-05010 and determined amino acid substitutions that emerged under the pressure of these compounds in the protease-encoding region. Finally, in view of the limited penetration of most antiviral drugs into the CNS, we evaluated the partition and distribution coefficients (log *P* and log *D*) as well as the apparent permeability coefficient (P_{app}) for blood-brain barrier (BBB) using an *in vitro* model, where we were able to demonstrate that GRL-04810 and GRL-05010 had potentially enhanced penetration capabilities across the BBB.

MATERIALS AND METHODS

Cells and viruses. MT-2 and MT-4 cells were grown in RPMI 1640-based culture medium supplemented with 10% fetal calf serum (FCS; JRH Biosciences, Lenexa, MD), 50 unit/ml penicillin, and 100 μg/ml of kanamycin. The following HIV-1 viruses were employed for the drug susceptibility assay (see below): HIV-1_{LAI}, HIV-1_{NL4-3}, the clinical HIV-1 strain HIV-$1_{ERS104pre}$ isolated from a drug-naive patient with AIDS (29), and six HIV-1 clinical isolates which were originally obtained from patients with AIDS who had received 9 to 11 anti-HIV-1 drugs over the past 32 to 83 months and which were genotypically and phenotypically characterized as multi-PI-resistant HIV-1 variants. All primary HIV-1 strains were passaged once or twice in 3-day-old phytohemagglutinin-activated peripheral blood mononuclear cells (PHA-PBMC), and the culture supernatants were stored at −80°C until use.

Antiviral agents. Saquinavir (SQV) was kindly provided by Roche Products, Ltd. (Welwyn Garden City, United Kingdom), and Abbott Laboratories (Abbott Park, IL). Amprenavir (APV) was received as a courtesy gift from Glaxo-Wellcome, Research Triangle Park, NC. Lopinavir (LPV) was kindly provided by Japan Energy, Inc., Tokyo, Japan. Atazanavir (ATV) was a contribution from Bristol-Myers Squibb (New York, NY). DRV was synthesized as previously described (30). 3′-Azido-2′,3′-dioxythymidine (AZT) was purchased from Sigma-Aldrich (St. Louis, MO). Indinavir (IDV) was kindly provided by Merck Research Laboratories (Rahway, NJ).

Drug susceptibility assay. The susceptibility of HIV-1_{LAI} to various drugs was determined as previously described, with minor modifications. Briefly, MT-2 cells (10^4/ml) were exposed to 100 50% tissue culture infectious doses ($TCID_{50}$) of HIV-1_{LAI} in the presence or absence of various concentrations of drugs in 96-well microculture plates and incubated at 37°C for 7 days. After 100 μl of the medium was removed from each well, 3-(4,5-dimetylthiazol-2-yl)-2,5-diphenyltetrazolium bromide (MTT) solution (10 μl; 7.5 mg/ml in phosphate-buffered saline) was added to each well in the plate, followed by incubation at 37°C for 2 h. After incubation, to dissolve the formazan crystals 100 μl of acidified isopropanol containing 4% (vol/vol) Triton X-100 was added to each well, and the optical density was measured in a kinetic microplate reader (VMax; Molecular Devices, Sunnyvale, CA). All assays were performed in duplicate or triplicate. In some experiments, MT-2 cells were chosen as target cells in the MTT assay since these cells undergo greater HIV-1-elicited cytopathic effects than MT-4 cells. To determine the sensitivity of primary HIV-1 isolates to drugs, phytohemagglutinin-stimulated peripheral blood mononuclear cells (PHA-PBMC) (10^6/ml) were exposed to 50 $TCID_{50}$ of each primary HIV-1 isolate and cultured in the presence or absence of various concentrations of drugs in 10-fold serial dilutions in 96-well microculture plates. In determining the drug susceptibility of certain laboratory HIV-1 strains, MT-4 cells were employed as target cells as previously described, with minor modifications. In brief, MT-4 cells (10^5/ml) were exposed to 100 $TCID_{50}$ of drug-resistant HIV-1 strains in the presence or absence of various concentrations of drugs and incubated at 37°C. On day 7 of culture, the supernatants were harvested, and the amounts of p24 Gag protein were determined by using a fully automated chemiluminescent enzyme immunoassay system (Lumipulse F; Fujirebio, Inc., Tokyo, Japan). Drug concentrations that suppressed the production of p24 Gag protein by 50% (50% effective concentration [EC_{50}]) were determined by comparison with the p24 production level in drug-free control cell culture. All assays were performed in duplicate or triplicate. PHA-PBMC were derived from a single donor in each independent experiment. Thus, to obtain the data, three different donors were recruited.

Generation of PI-resistant HIV-1 variants *in vitro*. MT-4 cells (10^5/ml) were exposed to HIV-1_{NL4-3} (500 $TCID_{50}$) and cultured in the presence of various PIs at an initial concentration equal to its EC_{50}. Viral replication was monitored by the determination of the amount of p24 Gag produced by MT-4 cells. The culture supernatants were harvested on day 7 and used to infect fresh MT-4 cells for the next round of culture in the presence of increasing concentrations of each drug. When the virus began to propagate in the presence of the drug, the drug concentration was increased generally 2- to 3-fold. Proviral DNA samples obtained from the lysates of infected cells were subjected to nucleotide sequencing. This drug selection procedure was carried out until the drug concentration reached 5 μM (31–33). In the experiments for selecting drug-resistant variants, MT-4 cells were exploited as target cells since HIV-1 in general replicates at greater levels in MT-4 cells than in MT-2 cells.

Determination of nucleotide sequences. Molecular cloning and determination of the nucleotide sequences of HIV-1 strains passaged in the presence of anti-HIV-1 agents were performed as described previously (31). In brief, high-molecular-weight DNA was extracted from HIV-1-infected MT-4 cells by using an InstaGene Matrix (Bio-Rad Laboratories, Hercules, CA) and subjected to molecular cloning, followed by sequence determination. The primers used for the first round of PCR with the entire Gag- and protease-encoding regions of the HIV-1 genome were LTR F1 (5′-GAT GCT ACA TAT AAG CAG CTG C-3′) and PR12 (5′-CTC GTG ACA AAT TTC TAC TAA TGC-3′). The first-round PCR mixture consisted of 1 μl of proviral DNA solution, 10 μl of Premix *Taq* (Ex *Taq* version; TaKaRa Bio, Inc., Otsu, Japan), and 10 pmol of each of the first PCR primers in a total volume of 20 μl. The PCR conditions used were an initial 3 min at 95°C, followed by 35 cycles of 40 s at 95°C, 20 s at 55°C, and 2 min at 72°C, with a final 10 min of extension at 72°C. The first-round PCR products (1 μl) were used directly in the second round of PCR with primers LTR F2 (5′-GAG ACT CTG GTA ACT AGA GAT C-3′) and Ksma2.1 (5′-CCA TCC CGG GCT TTA ATT TTA CTG GTA C-3′) under the PCR conditions of an initial 3 min at 95°C, followed by 35 cycles of 30 s at 95°C, 20 s at 55°C, and 2 min at 72°C, with a final 10 min of extension at 72°C. The second-round PCR products were purified with spin col-

umns (MicroSpin S-400 HR columns; Amersham Biosciences Corp., Piscataway, NJ), cloned directly, and subjected to sequencing with a model 3130 automated DNA sequencer (Applied Biosystems, Foster City, CA).

Determination of replication kinetics of GRL-04810- and GRL-05010-resistant HIV-1_{NL4-3} variants and wild-type HIV-1_{NL4-3}. GRL-04810- and GRL-05010-resistant variants were obtained at passages 18 and 10, respectively, and propagated in fresh MT-4 cells without the drugs for 7 days, and viral stocks were stored at −80°C until use. MT-4 cells (3×10^5) were exposed to the wild-type HIV-1_{NL4-3} preparation or HIV-1_{NL4-3} preparations selected with GRL-04810 over 18 passages and GRL-05010 over 10 passages, designated HIV-$1_{GRL\text{-}04810^{R}P18}$ and HIV-$1_{GRL\text{-}05010^{R}P10}$, respectively, containing 10 ng/ml p24, in six-well culture plates for 3 h. Such MT-4 cells were subsequently washed with fresh medium and divided into three fractions, each of which was cultured with or without each compound (final concentration of MT-4 cells, 10^4/ml; drug concentrations, 0.01 μM and 0.001 μM). The amounts of p24 were measured every 2 days for up to 7 days.

Determination of partition and distribution coefficients of GRL-04810 and GRL-05010 using the shake flask method. On day −1 of the experimental setting, saturation of 1-octanol [$CH_3(CH_2)_6CH_2OH$] (Nacalai Tesque, Kyoto, Japan) with water and Tris-buffered saline (10× working solution; 20 mM Tris, pH 7.4–0.9% NaCl [Sigma-Aldrich, St. Louis, MO]) took place. Four different flasks were used. One contained 50 ml of water plus 100 ml of 1-octanol, and another flask contained 1-octanol saturated with water by the addition of 50 ml of 1-octanol and 100 ml of water. For the other two flasks, the same ratios and volumes were kept for 1-octanol saturated with Tris buffer and Tris buffer saturated with 1-octanol. The flasks were sealed and placed in a Bioshaker at room temperature for 24 h at 90 rpm. Simultaneously, dilutions of GRL-04810, GRL-05010, and DRV were performed from a 20 mM dimethyl sulfoxide (DMSO) stock to a final concentration of 100 μM using distilled H_2O (dH_2O), Tris-buffered saline, and 1-octanol as solvents. Successive dilutions were made to obtain concentrations of 10 μM, 1 μM, and 0.1 μM. A standard curve was generated on a light spectrophotometer (DU Series 700; Beckman Coulter, Fullerton, CA) at an absorbance of 230.

On day 1 of the experiment, the lipid and liquid interfaces were separated, and compounds were diluted again from 20 mM DMSO to 100 μM using the 1-octanol, water, and Tris-buffered saline obtained from the shake flask assay. The resulting diluted compounds were then added to separate serum tubes containing equal proportions of 1-octanol and water and of 1-octanol and Tris-buffered saline. The solution was hand shaken for 5 min and then centrifuged at 3,500 rpm and room temperature for 20 min. Finally, the compounds were recovered from the 1-octanol, Tris buffer, and water interfaces and then measured on a light spectrophotometer.

The values for log *P* and log *D* were obtained according to the following mathematical formulas: $\log P_{octanol/water} = \log([compound]_{n\text{-}octanol}/[compound]_{water})$ and $\log D_{octanol/water} = \log([compound]_{n\text{-}octanol}/[compound]_{ionized} + /[compound]_{neutral})$, where $[compound]_{n\text{-}octanol}$, $[compound]_{water}$, $[compound]_{ionized}$, and $[compound]_{neutral}$ represent the concentrations of compound in *n*-octanol, water, ionized water, and neutral water, respectively.

Determination of the apparent permeability coefficients of GRL-04810 and GRL-05010 for the blood-brain barrier using a novel *in vitro* model. A novel *in vitro* BBB model (BBB Kit; PharmaCo-Cell, Ltd., Nagasaki, Japan), incorporating a triple culture of rat-derived astrocytes, pericytes, and monkey-derived endothelial cells (34) was used to determine the apparent permeability coefficient (P_{app} in cm/s) for the BBB of GRL-04810, GRL-05010, AZT, IDV, SQV, LPV, ATV, DRV, caffeine, and sucrose.

The BBB Kit was kept at −80°C until it was thawed on day 0 of the experiments. Nutritional medium was added to both brain and blood sides of the wells. This solution consists of Dulbecco's modified Eagle's medium (DMEM)/F-12 medium with 10% (vol/vol) FCS, 100 μg/ml heparin, 1.5 ng/ml basic fibroblast growth factor (bFGF), 5 μg/ml insulin, 5 μg/ml transferrin, 5 ng/ml sodium selenite, 500 nM hydrocortisone, and 50 μg/ml gentamicin. Fresh medium was added 3 h after thawing, following the manufacturer's instructions, and 24 h later. The plates were incubated at 37°C until day 4 of the experiment when the condition of astrocytes was checked under a light microscope. Following this, the integrity of the collagen-coated membrane was verified by the measurement of transendothelial electrical resistance (TEER) using an ohmmeter provided by the manufacturer. As TEER increases over time and reaches a peak between days 4 and 6 of the experiment, determinations were done during this period. Membranes were tested individually, and collagen-coated membranes displaying TEER values greater than 150 Ω/cm^2 were deemed suitable for the execution of the drug BBB penetration assay. Detailed information regarding the components of the BBB Kit as well as its mechanisms can be seen by accessing the manufacturer's website (PharmaCo-Cell, Nagasaki, Japan).

Once the conditions of cell viability and membrane integrity were met, drug dilutions were performed from 20 mM DMSO stocks of GRL-04810, GRL-05010, AZT, IDV, SQV, LPV, ATV, and DRV, while caffeine and sucrose were used as positive and negative controls, respectively. Standard curves were generated for each compound on a light spectrophotometer as previously described. Each compound (100 μM) was added to the luminal (blood) side of the wells and incubated at 37°C for 30 min, and then the amount of drug that crossed the *in vitro* BBB was collected and measured under a light spectrophotometer at an absorbance of 230.

P_{app} was calculated using the following mathematical formula: P_{app} (cm/s) = $(VA/A \times [C]_{luminal}) \times (\Delta[C]_{abluminal}/\Delta t)$, where VA is the volume of the abluminal chamber (0.9 cm^3), *A* is the membrane surface area (0.33 cm^2), $[C]_{luminal}$ is the initial luminal compound concentration (μM), $\Delta[C]_{abluminal}$ is the abluminal compound concentration (μM), and Δt is the time of the experiment (seconds).

Determination of antiviral activities of GRL-04810, GRL-05010, and DRV recovered from the brain side of the BBB assay. Each drug that successfully crossed the brain interface in the BBB assay described above was harvested; these drugs were designated GRL-04810^{brain}, GRL-05010^{brain}, DRV^{brain}, AZT^{brain}, IDV^{brain}, and SQV^{brain}. The susceptibility of HIV-1_{LAI} and HIV-$1_{ERS104pre}$ to GRL-04810^{brain}, GRL-05010^{brain}, DRV^{brain}, AZT^{brain}, IDV^{brain}, and SQV^{brain} was then determined in an MTT assay using MT-2 cells or a p24 assay employing PHA-PBMC as described in the drug susceptibility assay section. The assay was carried out using brain-side stocks of compounds diluted 10-, 100-, 1,000-, and 10,000-fold.

Structural interactions of GRL-04810 and GRL-05010 with wild-type HIV-1 protease. Molecular models of the interactions of GRL-04810 and GRL-05010 with wild-type HIV-1 protease were generated as follows. The coordinates of the structure of a reference compound, GRL-0519, with HIV-1 protease were obtained from the Protein Data Bank (PDB code 3OK9 [http://www.rcsb.org/]). GRL-0519 shares structural similarity with GRL-04810, and its structure was modified to generate the molecular model of interactions of GRL-04810 and HIV-1 protease. The complex was energy minimized using OPLS-2005 force field as implemented in Maestro (version 9.3; Schrödinger, LLC, New York, NY). A model of the interactions of GRL-05010 with HIV-1 protease was obtained in a similar fashion using the crystal structure of darunavir with protease (PDB code 2IEN) as a reference. Visualization, analyses of the models, and figures depicting structural interactions were generated using Maestro.

RESULTS

Antiviral activity of GRL-04810 and GRL-05010 against HIV-1_{LAI}. We designed and synthesized GRL-04810 and GRL-05010 that contain two fluorine atoms in the *bis*-THF moiety (Fig. 1) and examined their antiviral activities against a variety of HIV-1 isolates. We found that GRL-04810 and GRL-05010 were highly active *in vitro* against a wild-type laboratory HIV-1 strain, HIV-1_{LAI}, with EC_{50}s of 0.0008 and 0.003 μM, respectively, as examined

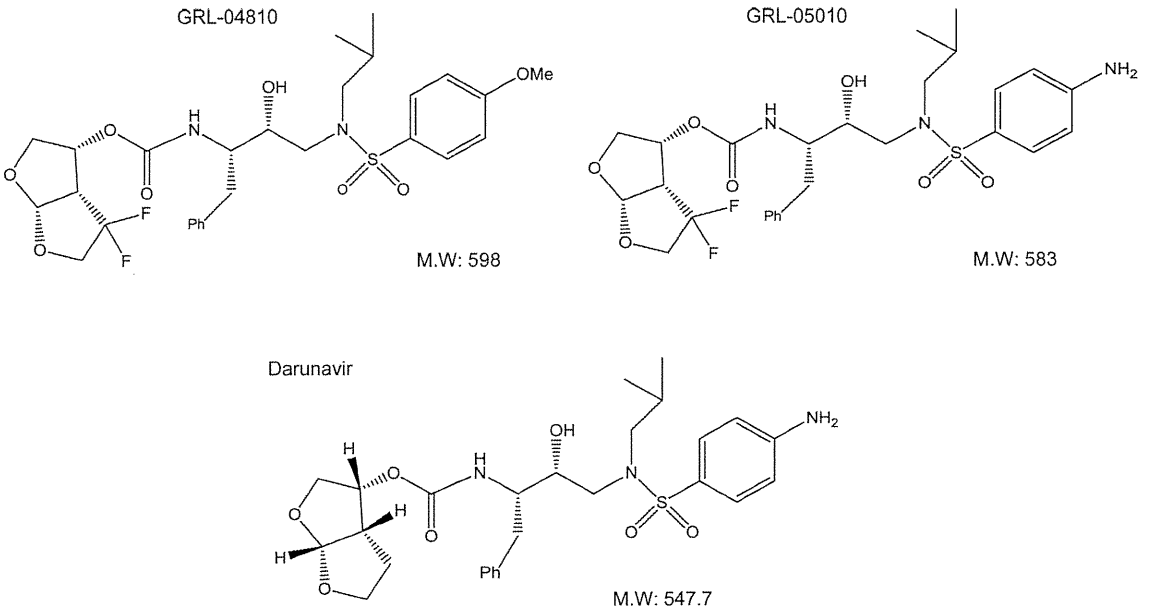

FIG 1 Structures of GRL-04810, GRL-05010, and darunavir. MW, molecular weight.

using an MTT assay with MT-2 as target cells, while FDA-approved PIs (SQV, LPV, ATV, APV, and DRV) displayed EC_{50}s ranging from 0.005 to 0.03 μM (Table 1). Cytotoxicity was seen for GRL-04810 and GRL-05010 only at high concentrations, with CC_{50} values of 17.5 and 37.0 μM; the selectivity index proved to be high for GRL-04810 at 21,875, while GRL-05010 scored a moderate selectivity index of 12,333 (Table 1).

GRL-04810 and GRL-05010 exert efficacious activity against highly PI-resistant clinical HIV-1 isolates. In our previous work, we isolated highly multi-PI-resistant primary HIV-1 strains, HIV-$1_{MDR/B}$ (where MDR is multidrug resistant), HIV-$1_{MDR/C}$, HIV-$1_{MDR/G}$, HIV-$1_{MDR/TM}$, HIV-$1_{MDR/JSL}$, and HIV-$1_{MDR/MM}$, from patients with AIDS who had failed then-existing anti-HIV regimens after receiving 9 to 11 anti-HIV-1 drugs over 32 to 83 months (35). These primary strains contained 9 to 14 amino acid substitutions in the protease-encoding region that have reportedly been associated with HIV-1 resistance against various PIs (substitutions are identified in the footnote of Table 2). The EC_{50}s of SQV, LPV, ATV, and APV against clinical multidrug-resistant HIV-1 strains were significantly higher than those against a wild-type clinical HIV-1 isolate, HIV-$1_{ERS104pre}$, as examined in the assay employing PHA-PBMC as target cells and using p24 production inhibition as an endpoint. However, GRL-04810 and GRL-05010 exerted efficient antiviral activities, and their EC_{50}s against those clinical variants were substantially low, varying from 0.002 μM to 0.021 μM (Table 2). GRL-04810 and GRL-05010 proved to be more active against all six multidrug-resistant clinical HIV-1 variants examined than all of the currently available approved PIs examined. The activities of the two compounds were comparable to or greater than the activity of DRV against the variants (Table 2).

TABLE 1 Antiviral activity of GRL-04810 and GRL-05010 against HIV-1_{LAI} and their cytotoxicities[a]

Compound	EC_{50} (μM)	CC_{50} (μM)	Selectivity index[b]
SQV	0.021 ± 0.001	17.7 ± 3.4	843
LPV	0.020 ± 0.001	26.8 ± 0.9	1,340
ATV	0.005 ± 0.001	28.6 ± 0.9	5,720
APV	0.03 ± 0.001	>100	>3,333
DRV	0.005 ± 0.001	>100	>20,000
GRL-04810	0.0008 ± 0.0002	17.5 ± 0.9	21,875
GRL-05010	0.003 ± 0.001	37.0 ± 0.4	12,333

[a] MT-2 cells (10^4/ml) were exposed to 100 $TCID_{50}$ of HIV-1_{LAI} and cultured in the presence of various concentrations of each PI, and the EC_{50}s were determined by MTT assay. All assays were conducted in duplicate, and the data shown represent mean values derived from the results of three independent experiments.

[b] Each selectivity index denotes a ratio of the CC_{50} to EC_{50} against HIV-1_{LAI}.

GRL-04810 and GRL-05010 are effective against PI-selected laboratory HIV-1 variants. We also examined GRL-04810 and GRL-05010 against a variety of HIV-1_{NL4-3} variants selected *in vitro* with each of four FDA-approved PIs (SQV, LPV, ATV, and APV). Such variants were selected by propagating HIV-1_{NL4-3} in the presence of increasing concentrations of each PI (up to 5 μM) in MT-4 cells (31); these variants had acquired various PI resistance-associated amino acid substitutions in the protease-encoding region of the viral genomes (substitutions are identified in the footnote of Table 3). These variants were designated HIV-$1_{SQV}{}^{R}{}_{5\ \mu M}$, HIV-$1_{LPV}{}^{R}{}_{5\ \mu M}$, HIV-$1_{ATV}{}^{R}{}_{5\ \mu M}$, and HIV-$1_{APV}{}^{R}{}_{5\ \mu M}$, with the superscript indicating the drug each of the variants was selected against. Each of the variants was highly resistant to the very PI against which the variant was selected and showed significant resistance, with EC_{50}s of >1 μM. GRL-04810 and GRL-05010 were generally as active against HIV-$1_{SQV}{}^{R}{}_{5\ \mu M}$, HIV-$1_{LPV}{}^{R}{}_{5\ \mu M}$, and HIV-$1_{ATV}{}^{R}{}_{5\ \mu M}$ as DRV (Table 3) when the absolute EC_{50}s were compared (Table 3). As in the case of DRV, the two compounds were less active against HIV-$1_{APV}{}^{R}{}_{5\mu M}$, with EC_{50}s of 0.43 and 0.56 μM, respectively, presumably due to their structural resemblance to APV.

GRL-04810 and GRL-0510 are moderately active against highly DRV-resistant HIV-1 variants. We also examined the an-

TABLE 2 Antiviral activity of GRL-04810 and GRL-05010 against multidrug-resistant clinical isolates in PHA-PBMC

Virus (tropism)[a]	EC_{50} (μM)[b]						
	SQV	LPV	ATV	APV	DRV	GRL-04810	GRL-05010
HIV-$1_{ERS104pre}$ (X4)	0.0039 ± 0.0001	0.033 ± 0.003	0.0021 ± 0.0001	0.0295 ± 0.0004	0.004 ± 0.001	0.0023 ± 0.0001	0.0027 ± 0.0003
HIV-$1_{MDR/B}$ (X4)	0.35 (90) ± 0.01	>1 (>33)	0.45 (214) ± 0.07	0.49 (15) ± 0.05	0.021 (5) ± 0.001	0.014 (7) ± 0.001	0.011 (3) ± 0.001
HIV-$1_{MDR/C}$ (X4)	0.31 (78) ± 0.02	>1 (>33)	0.43 (204) ± 0.01	0.21 (7) ± 0.02	0.005 (1) ± 0.001	0.002 (1) ± 0.001	0.002 (1) ± 0.001
HIV-$1_{MDR/G}$ (X4)	0.039 (10) ± 0.002	>1 (>33)	0.042 (19) ± 0.001	0.31 (11) ± 0.08	0.014 (4) ± 0.009	0.004 (2) ± 0.001	0.004 (1) ± 0.001
HIV-$1_{MDR/TM}$ (X4)	0.10 (25) ± 0.04	>1 (>33)	0.056 (24) ± 0.007	0.328 (12) ± 0.001	0.03 (9) ± 0.01	0.004 (2) ± 0.001	0.004 (2) ± 0.001
HIV-$1_{MDR/JSL}$ (R5)	0.53 (133) ± 0.01	>1 (>33)	>1 (>476)	0.630 (22) ± 0.009	0.025 (5) ± 0.002	0.021 (10) ± 0.004	0.020 (7) ± 0.0002
HIV-$1_{MDR/MM}$ (R5)	0.11 (27) ± 0.01	>1 (>33)	0.081 (38) ± 0.008	0.27 (9) ± 0.01	0.010 (3) ± 0.001	0.002 (1) ± 0.001	0.003 (1) ± 0.001

[a] The amino acid substitutions identified in the protease-encoding region compared to the consensus type B sequence cited from the Los Alamos database include L63P in HIV-$1_{ERS104pre}$; L10I, K14R, L33I, M36I, M46I, F53I, K55R, I62V, L63P, A71V, G73S, V82A, L90M, and I93L in HIV-$1_{MDR/B}$; L10I, I15V, K20R, L24I, M36I, M46L, I54V, I62V, L63P, K70Q, V82A, and L89M in HIV-$1_{MDR/C}$; L10I, V11I, T12E, I15V, L19I, R41K, M46L, L63P, A71T, V82A, and L90M in HIV-$1_{MDR/G}$; L10I, K14R, R41K, M46L, I54V, L63P, A71V, V82A, L90M, and I93L in HIV-$1_{MDR/TM}$; L10I, L24I, I33F, E35D, M36I, N37S, M46L, I54V, R57K, I62V, L63P, A71V, G73S, and V82A in HIV-$1_{MDR/JSL}$; L10I, K43T, M46L, I54V, L63P, A71V, V82A, L90M, and Q92K in HIV-$1_{MDR/MM}$. HIV-$1_{ERS104pre}$ served as a source of wild-type HIV-1.

[b] The EC_{50} values were determined by using PHA-PBMC as target cells, and the inhibition of p24 Gag protein production by each drug was used as an endpoint. The numbers in parentheses represent the fold changes of EC_{50}s for each isolate compared to the EC_{50}s for wild-type HIV-$1_{ERS104pre}$. All assays were conducted in duplicate or triplicate, and the data shown represent mean values (± 1 standard deviation) derived from the results of three independent experiments. PHA-PBMC were derived from a single donor in each independent experiment.

tiviral activity of the two compounds against DRV-resistant variants, which we previously selected out *in vitro* against DRV (36). These variants were generated using a mixture of eight highly multi-PI-resistant clinical isolates as a starting HIV-1 population and were selected with increasing concentrations of DRV. GRL-04810 and GRL-05010 exhibited slightly decreased activity against variants selected with DRV over 10 and 20 passages (EC_{50}s of 0.03 to 0.034 μM for the former and 0.026 to 0.043 μM for the latter) (see Table S1 in the supplemental material), while DRV was less active against HIV-$1_{DRV^R_{P20}}$ than the two compounds, with an EC_{50} of 0.174 μM (see Table S1).

***In vitro* selection of HIV-1 variants resistant to GRL-04810 and GRL-05010.** We attempted to select HIV-1 variants with GRL-04810 and GRL-05010 by propagating a laboratory HIV-1 strain, HIV-1_{NL4-3}, in MT-4 cells in the presence of increasing concentrations of each of the two drugs, as previously described (31). HIV-1_{NL4-3} was exposed to GRL-04810 with an initial concentration of 0.003 μM and underwent 25 passages when the virus had acquired an ability to replicate in the presence of a 26-fold-increased concentration of GRL-04810 (0.080 μM). A selection assay was also carried out for GRL-05010 starting at 0.003 μM. (Fig. 2), and HIV-1_{NL4-3} attained an ability to replicate in the presence of 0.037 μM GRL-05010 by passage 15.

Judging from the amounts of p24 Gag protein secreted into the culture medium, the replicative capacity of HIV-1_{NL4-3} at passages 25 and 15 for GRL-04810 and GRL-05010, respectively, was generally maintained. We compared whether the emergence of resistance-associated amino acid substitutions in GRL-04810- and GRL-05010-exposed HIV-1_{NL4-3} was delayed in comparison with the emergence of resistant variants against two commercially available FDA-approved PIs (LPV and DRV). The protease-encoding region of proviral DNA isolated from MT-4 cells was cloned and sequenced at passages 5, 10, 15, and 20 during the GRL-04810 selection and at passages 5, 10, and 15 for GRL-05010. HIV-1_{NL4-3} exposed to GRL-04810 by passage 20 had acquired L33F and V82I in 15 of 22 clones and A28S in 5 clones. HIV-1_{NL4-3} exposed to GRL-05010 had acquired amino acid substitutions M46I and I50V by passage 15 in all 24 clones examined, while

TABLE 3 Antiviral activity of GRL-04810 and GRL-05010 against laboratory PI-resistant HIV-1 variants and GRL-04810- and GRL-05010-exposed HIV-1 variants

Virus[a]	EC_{50} (μM)[b]						
	SQV	LPV	ATV	APV	DRV	GRL-04810	GRL-05010
HIV-1_{NL4-3}	0.037 ± 0.002	0.035 ± 0.005	0.0047 ± 0.0001	0.081 ± 0.001	0.004 ± 0.001	0.0005 ± 0.0005	0.0037 ± 0.0001
HIV-$1_{SQV^R_{5\mu M}}$	>1 (>25)	>1 (>25)	>1 (>250)	0.435 (5) ± 0.001	0.04 (10) ± 0.01	0.13 (260) ± 0.05	0.046 (13) ± 0.001
HIV-$1_{LPV^R_{5\mu M}}$	0.025 (1) ± 0.005	>1 (>25)	0.033 (8) ± 0.001	0.033 (1) ± 0.005	0.032 (8) ± 0.001	0.03 (66) ± 0.01	0.03 (8) ± 0.02
HIV-$1_{ATV^R_{5\mu M}}$	0.46 (12) ± 0.02	>1 (>25)	> 1 (>250)	>1 (>13)	0.05 (13) ± 0.01	0.02 (36) ± 0.01	0.04 (12) ± 0.02
HIV-$1_{APV^R_{5\mu M}}$	0.09 (2) ± 0.04	>1 (>25)	0.66 ± 0.02	>1 (>13)	0.51 (128) ± 0.03	0.43 (860) ± 0.02	0.56 (187) ± 0.03
HIV-$1_{GRL04810^R_{P18}}$	0.032 (1) ± 0.005	0.37 (11) ± 0.02	0.325 (81) ± 0.004	>1 (>13)	0.041 (11) ± 0.001	0.033 (66) ± 0.003	0.039 (13) ± 0.005
HIV-$1_{GRL05010^R_{P10}}$	0.036 (1) ± 0.003	0.375 (11) ± 0.005	0.095 (24) ± 0.035	>1 (>13)	0.037 (10) ± 0.003	0.029 (58) ± 0.001	0.036 (10) ± 0.001

[a] The amino acid substitutions identified in the protease-encoding region compared to the wild-type HIV-1_{NL4-3} include L10F, V32I, M46I, I54M, A71V, and I84V in HIV-$1_{APV^R_{5\mu M}}$; L23I, E34Q, K43I, M46I, I50L, G51A, L63P, A71V, V82A, and T91A in HIV-$1_{ATV^R_{5\mu M}}$; L10F, M46I, I54V, and V82A in HIV-$1_{LPV^R_{5\mu M}}$; and L10I, G48V, I54V, A71V, I84V, and L90M in HIV-$1_{SQV^R_{5\mu M}}$.

[b] MT-4 cells (10^5/ml) were exposed to 100 $TCID_{50}$ of each HIV-1, and the inhibition of p24 Gag protein production by each drug was used as an endpoint. The numbers in parentheses represent the fold changes of EC_{50}s for each isolate compared to the EC_{50}s for wild-type HIV-1_{NL4-3}. All assays were conducted in duplicate or triplicate, and the data shown represent mean values (± 1 standard deviation) derived from the results of two or three independent experiments. In addition, GRL-04810- and GRL-05010-resistant variants selected *in vitro* were used for antiviral activity determination assays. Time point viruses were harvested at passages 18 and 10, respectively. Washing steps were performed to remove the remaining compounds from the viral stocks, and compound-free viruses were obtained for the experiment. Five commercially available protease inhibitors were used as controls. Absolute values are given plus the fold changes relative to the baseline EC_{50} for each compound. By passage 18, three amino acid substitutions A28S, L33F, and V82I were identified in HIV-$1_{GRL04810^R_{P18}}$; by passage 10, M46I, I50V, N38K, and M36I were detected in HIV-$1_{GRL05010^R_{P10}}$. Assays were performed in duplicate and the average values (with 1 standard deviation) are shown.

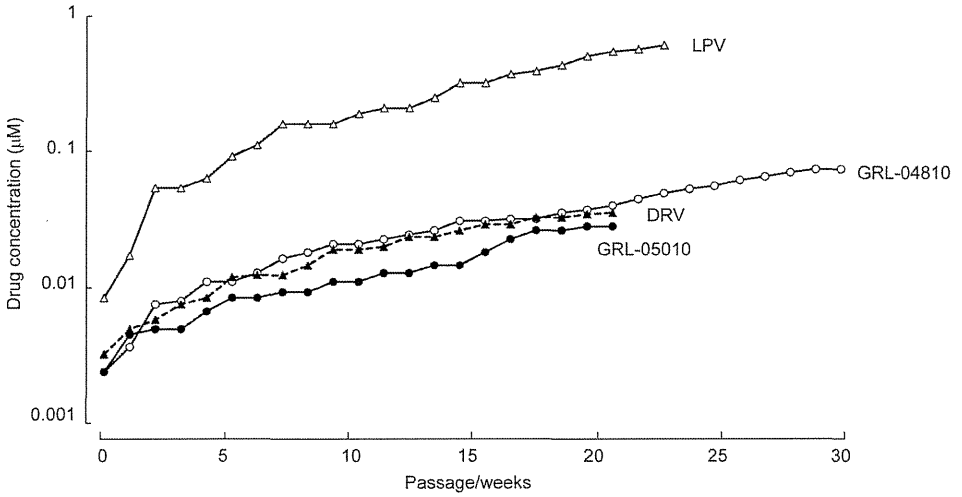

FIG 2 Selection of *in vitro* variants resistant to GRL-04810 and GRL-05010. MT-4 cells were exposed to the wild-type strain HIV-1_{NL4-3} and cultured in the presence of increasing concentrations of GRL-04810, GRL-05010, DRV, and LPV. Culture supernatants were collected weekly, and if the amounts of p24 Gag were found to surpass the cutoff value of 200 ng/ml, those supernatants were used for the subsequent passage. Each passage was conducted in a cell-free manner.

N38K was detected in 8 of 24 clones, and M36I was found in 3 clones (Fig. 3).

GRL-04810- and GRL-05010-resistant HIV-1_{NL4-3} variants maintain robust replicative activity. We determined the replication kinetics of HIV-$1_{GRL-04810}{}^{R}{}_{P18}$, HIV-$1_{GRL-05010}{}^{R}{}_{P10}$, and the wild-type HIV-$1_{NL4-3}$ using replication kinetics assays as previously described (31). HIV-1_{NL4-3} replicated well in the presence of 0.001 μM each of the two compounds, but was delayed in starting to replicate or failed to replicate in the presence of 0.01 μM each compound in the 7-day replication kinetics assay (Fig. 4). However, HIV-$1_{GRL-04810}{}^{R}{}_{P18}$ and HIV-$1_{GRL-05010}{}^{R}{}_{P10}$ robustly replicated in the presence of 0.001 and 0.01 μM each of the two compounds (Fig. 4).

GRL-04810 and GRL-05010 remain active against the variants selected with GRL-04810 and GRL-05010. We then attempted to determine the impact of the amino acid substitutions identified in HIV-$1_{GRL-04810}{}^{R}{}_{P18}$ and HIV-$1_{GRL-05010}{}^{R}{}_{P10}$. Five commercially available protease inhibitors (SQV, LPV, ATV, APV, and DRV) were used as controls. GRL-04810 and GRL-05010 generally remained active against HIV-$1_{GRL-04810}{}^{R}{}_{P18}$ and HIV-$1_{GRL-05010}{}^{R}{}_{P10}$, with EC_{50}s ranging from 0.029 μM to 0.039 μM. SQV was active against the two variants HIV-$1_{GRL-04810}{}^{R}{}_{P18}$ and HIV-$1_{GRL-05010}{}^{R}{}_{P10}$, with narrow EC_{50} ranges of 0.032 to 0.036 μM, while LPV displayed values significantly higher (0.37 and 0.375 μM) than those of GRL-04810 and GRL-05010. ATV was moderately active against the HIV-$1_{GRL-05010}{}^{R}{}_{P10}$ variant (0.095 μM), while the absolute EC_{50}s of GRL-04810 and GRL-05010 were generally lower than the EC_{50}s of ATV against those variants. As for DRV, the values against the variants resistant to GRL-04810 and GRL-05010 were 0.041 and 0.037 μM, respectively. However,

```
                          10        20        30        40        50        60        70        80        90        99
pNL4-3  PR    PQITLWQRPL VTIKIGGQLK EALLDTGADD TVLEEMNLPG RWKPKMIGGI GGFIKVRQYD QILIEICGHK AIGTVLVGPT PVNIIGRNLL TQIGCTLNF

HIV-1GRL-04810 P20 ..........  ..........  ..........  ..F.......  ..........  ..........  ..........  ..........  .I........  .........  7/22
                   ..........  ..........  ..........  ..........  ..........  ..........  ..........  ..........  ..........  .........  6/22
                   ..........  ..........  .......S..  ..F.......  ..........  ..........  ..........  ..........  .I........  .........  5/22
                   ..........  ..........  ..........  ..F.......  ..........  ..........  ..........  ..........  .I........  ....R....  1/22
                   ..........  ..........  ..........  ..........  ..........  ..........  ..........  ..........  .I........  .........  1/22
                   ..........  ..........  ..........  ..F.......  ..........  ..........  ..........  ..........  ..........  .........  1/22
                   ..........  ..........  ...F......  ..F.......  ..........  ..........  ..........  ..........  .I........  .........  1/22

HIV-1GRL-05010 P15 ..........  ..........  ..........  ..........  .....I...V  ..........  ..........  ..........  ..........  .........  11/24
                   ..........  ..........  ..........  ......K...  .....I...V  ..........  ..........  ..........  ..........  .........  8/24
                   ..........  ..........  ..........  .....I....  .....I...V  ..........  ..........  ..........  ..........  .........  3/24
                   ..........  ..........  ..........  ..........  .....I...V  .....A....  ..........  ..........  ..........  .........  1/24
                   ..........  ......V...  ..........  ..........  .....I...V  ..........  ..........  ..........  ..........  .........  1/24

HIVDRV P20         ..........  ..........  ..........  ..........  ..........  ..........  ..........  ..........  ..........  .........  20/20
```

FIG 3 Amino acid sequences of the protease-encoding region of HIV-1 variants selected in the presence of GRL-04810 and GRL-05010. Shown are the amino acid sequences deduced from the nucleotide sequences of the protease-encoding region of proviral DNA isolated from HIV-1_{NL4-3} variants selected in the presence of GRL-04810, GRL-05010, and DRV at passages 20, 15, and 20, respectively. Identified amino acid substitutions in the protease-encoding region and their frequencies (far-right column) are shown. The amino acid sequence of the wild-type HIV-1_{NL4-3} protease (pNL4-3 PR) is shown at the top as a reference.

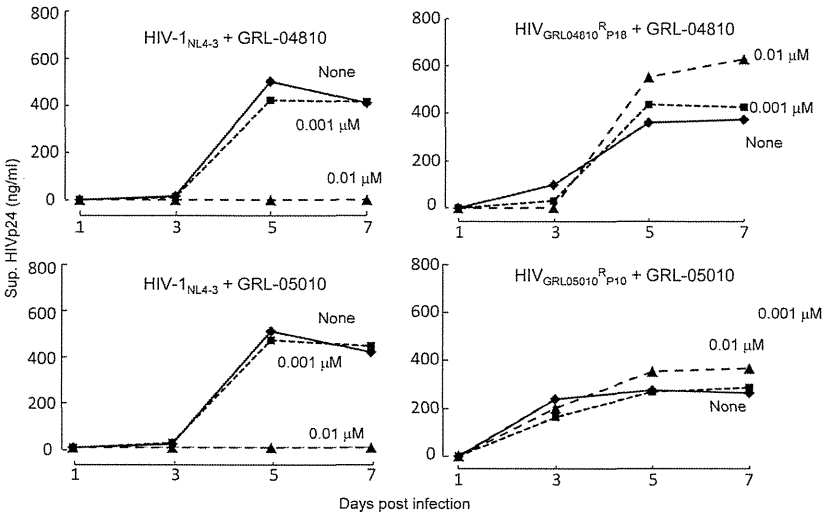

FIG 4 Replication kinetics of GRL-04810- and GRL-05010-resistant HIV-1 variants generated *in vitro*. GRL-04810- and GRL-05010-resistant viruses were obtained from the selection assay illustrated in Fig. 2. Two time point passages, HIV-$1_{GRL-04810}{}^{R}{}_{P18}$ and HIV-$1_{GRL-05010}{}^{R}{}_{P10}$, were chosen. HIV-$1_{NL4-3}$ or two resistant viruses were propagated in $CD4^+$ MT-4 cells in the presence of 0.01 μM (▲) and 0.001 μM (■) GRL-04810 and GRL-05010 or in the absence (◆) of the compounds in culture flasks. The amounts of p24 in each culture flask were quantified every 2 days for 1 week. Sup, supernatant.

APV was not active against any of the selected variants examined (EC_{50}s of >1 μM), presumably due to its structural resemblance to the two PIs used for the selection (Table 3).

GRL-04810 and GRL-05010 show favorable lipophilicity indexes for their partition and distribution coefficients. The addition of fluorine atoms is generally expected to confer greater lipophilicity on nucleoside analogs and certain compounds (37–39). Thus, we determined the partition (log *P*) and distribution (log *D*) coefficients of GRL-04810 and GRL-05010. 1-Octanol, organic alcohol, and water were used for log *P* determination, while Tris-buffered saline (pH 7.4) and water were utilized for log *D* determination. Prior to obtaining the actual values, a standard curve was generated as a reference, and drug concentrations attained for each compartment (1-octanol, water, and Tris-buffered saline) were measured on a light spectrophotometer (at an absorbance of 230 nm) as previously described by Rak et al. (40). Of note, GRL-04810 reached the highest concentration in the octanol lipid interface (72 μM) versus 14.09 μM for GRL-05010 and 11.89 μM for DRV (Table 4). GRL-04810 appeared the most lipophilic, with a log *D* value of −0.29, representing a 4-fold greater log *D* value than that of DRV (−1.03), since the assumption is that the more negative the log *D* value is, the less lipophilic the substance is estimated to be (40). GRL-05010 was found to have a log *D* value (−1.01) comparable to that of DRV.

GRL-04810 and GRL-05010 penetrate well across the blood-brain barrier *in vitro*. We also attempted to evaluate whether GRL-04810 and GRL-05010 had optimal blood-brain barrier (BBB) apparent permeability coefficients by employing an *in vitro* model using a triple cell coculture system with rat astrocytes, pericytes, and monkey endothelial cells. This model (BBB Kit) is thought to represent an *in vitro* BBB model for drug transport assays, permitting adequate cross talk of the cell lines involved and providing a way to test apparent passage of small molecules across the BBB, as previously described by Nakagawa et al. (41). AZT, IDV, SQV, LPV, ATV DRV, GRL-04810, or GRL-05010 was added to the luminal interface (termed the blood side) of microtiter culture wells under the optimal conditions for transendothelial electrical resistance (TEER) determination. The concentrations of each compound that permeated into the abluminal interface (termed the brain side) were determined using a spectrophotometer 30 min after the addition of each drug to the wells. As shown in Table 5, the amounts of caffeine and sucrose, serving as the most and least lipophilic substances, in the abluminal interface were 6.60 and 0.03 μM, respectively. AZT, IDV, SQV, LPV, ATV, and DRV were also used as controls in the assay, giving amounts of 1.50, 2.42, 0.33, 0.94, 1.02, and 0.65 μM, respectively. In contrast, GRL-04810 and GRL-05010 yielded greater concen-

TABLE 4 Partition and distribution coefficients of GRL-04810, GRL-05010, and DRV using the shake flask method

Compound	Concn (μM) in:				Log $P_{octanol/water}$[a]	Log $D_{octanol/Tris}$[a]
	Water	Tris buffer	*n*-Octanol	*n*-Octanol		
GRL-04810	99.78	42.32	70.00	72.00	−0.14	−0.29
GRL-05010	94.55	49.84	18.70	14.09	−0.83	−1.01
DRV	81.49	48.77	15.50	11.89	−0.63	−1.03

[a] The partition (log *P*) and distribution (log *D*) coefficients of GRL-04810 and GRL-05010 were determined. DRV was used as a control. *n*-Octanol, an organic alcohol, and water were used for log *P* determination, while Tris buffer (pH 7.40) and octanol were utilized for the log *D* assay. Prior to the retrieval of actual values, a standard curve was generated as a reference. The drug concentrations for each compartment (octanol, water, and Tris buffer) were measured at an absorbance of 230 using a light spectrophotometer. Assays were performed following the OECD guidelines for testing of chemicals (55). Log *P* and log *D* values were calculated according to the formulas given in Materials and Methods.

TABLE 5 Estimation of the apparent blood brain barrier permeability coefficient using an *in vitro* model[a]

Compound	Initial luminal tracer concn (μM)	Final abluminal tracer concn (μM)	P_{app} (10^{-6} cm/s)
AZT	100	1.50 ± 0.12	22.7 ± 1.9
IDV	100	2.42 ± 0.12	36.7 ± 1.7
SQV	100	0.33 ± 0.03	4.9 ± 0.4
LPV	100	0.94 ± 0.05	14.2 ± 0.7
ATV	100	1.02 ± 0.10	15.4 ± 1.4
DRV	100	0.65 ± 0.23	9.9 ± 4.2
GRL-04810	100	3.16 ± 0.48	47.8 ± 8.8
GRL-05010	100	4.08 ± 0.65	61.8 ± 12.1
Caffeine	100	6.60	100
Sucrose	100	0.03 ± 0.005	0.33 ± 0.13

[a] In the *in vitro* model using a triple coculture of rat astrocytes, pericytes, and monkey endothelial cells, AZT, IDV, SQV, LPV, ATV, DRV, GRL-04810, GRL-05010 (all 100 μM), and the positive and negative controls, caffeine and sucrose, respectively, were added to the luminal interface (termed blood side) of duplicate wells. The mathematical formula used for the calculation of P_{app} is described in Materials and Methods. Results show average values ±1 standard deviation of duplicate determinations.

trations, with 3.16 and 4.08 μM in the abluminal interface of the microtiter culture wells.

The apparent permeability coefficient (P_{app}), referred to as a brain uptake index (BUI), is a way to determine the penetration efficiency of a compound across a BBB model quantitatively and qualitatively (42). The P_{app} values of GRL-04810 (47.8×10^{-6} cm/s) and GRL-05010 (61.8×10^{-6} cm/s) were significantly greater than the P_{app} of DRV (9.9×10^{-6} cm/s) and the P_{app} values of other antiviral drugs tested: AZT (22.7×10^{-6} cm/s), IDV (36.7×10^{-6} cm/s), SQV (4.9×10^{-6} cm/s), LPV (14.2×10^{-6} cm/s), and ATV (15.4×10^{-6} cm/s). Compounds with apparent permeability coefficients greater than 20×10^{-6} cm/s are thought to have reasonably efficient penetration across the BBB; those with values of 10×10^{-6} to 20×10^{-6} cm/s have a moderate degree of penetration, whereas those with values lower than 10×10^{-6} cm/s do not penetrate the BBB well (41).

GRL-04810 and GRL-05010 recovered from the brain interface in the BBB model retain antiviral activity greater than that of DRV. Finally, we attempted to examine whether the drug concentrations penetrated into the abluminal interface (brain side) in the BBB Kit as described above had sufficient activity to suppress the replication of HIV-1 *in vitro*. Each drug that successfully crossed the brain interface in the BBB assay was harvested; these drugs were designated GRL-04810^{brain}, GRL-05010^{brain}, DRV^{brain}, AZT^{brain}, IDV^{brain}, and SQV^{brain}. The susceptibility of HIV-1_{LAI} and HIV-$1_{ERS104pre}$ to GRL-04810^{brain}, GRL-05010^{brain}, DRV^{brain}, AZT^{brain}, IDV^{brain}, and SQV^{brain} was then determined in MTT assays using MT-2 cells or in p24 assays employing PHA-PBMC as described in the drug susceptibility assay section. In the assay, we used 10-fold serial dilutions of the original brain side preparation containing GRL-04810 (3.16 μM) (designated GRL-04810^{brain}) and determined antiviral suppression levels. The 10-fold-diluted GRL-04810^{brain} (concentration, 0.316 μM) suppressed HIV-1_{LAI} replication by 94%, whereas 100-fold-diluted GRL-04810^{brain} (concentration, 0.0316 μM) suppressed replication by 45%. The 10-fold-diluted GRL-05010^{brain} (concentration, 0.408 μM) suppressed HIV-1_{LAI} replication by 91%, whereas 100-fold-diluted GRL-05010^{brain} (concentration, 0.0316 μM) suppressed replication by 73%. However, the suppression levels of all of the other preparations examined (DRV^{brain}, AZT^{brain}, IDV^{brain}, and SQV^{brain}) were less than those of GRL-04810^{brain} and GRL-05010^{brain} (Fig. 5). When PHA-activated PBMC and the treatment-naive clinical isolate HIV-$1_{ERS104pre}$ were used in the drug

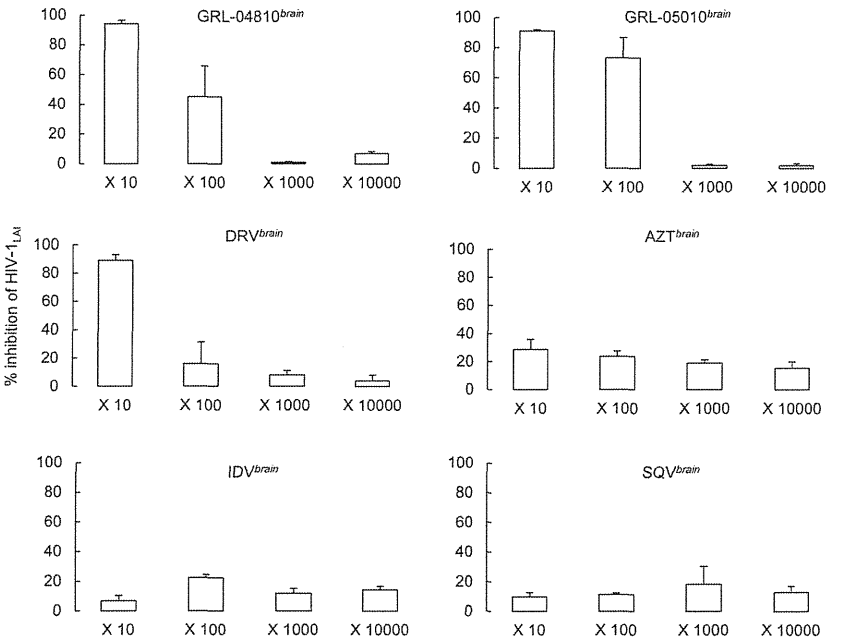

FIG 5 Antiviral activity of GRL-04810^{brain}, GRL-05010^{brain}, DRV^{brain}, AZT^{brain}, IDV^{brain} and SQV^{brain} against HIV-1_{LAI}. Compounds recovered from the brain side of the medium in the BBB *in vitro* assay were challenged with HIV-1_{LAI}, as indicated, in a p24 assay using PHA-PBMC. Dilution ranges were between 10-fold and 10,000-fold, and the percentage of viral inhibition was used as an endpoint. It is assumed that the greater the percentage of inhibition of HIV-1_{LAI}, the greater the concentration of the drug in the brain side medium. Assays were conducted in duplicate, and error bars show standard deviations.

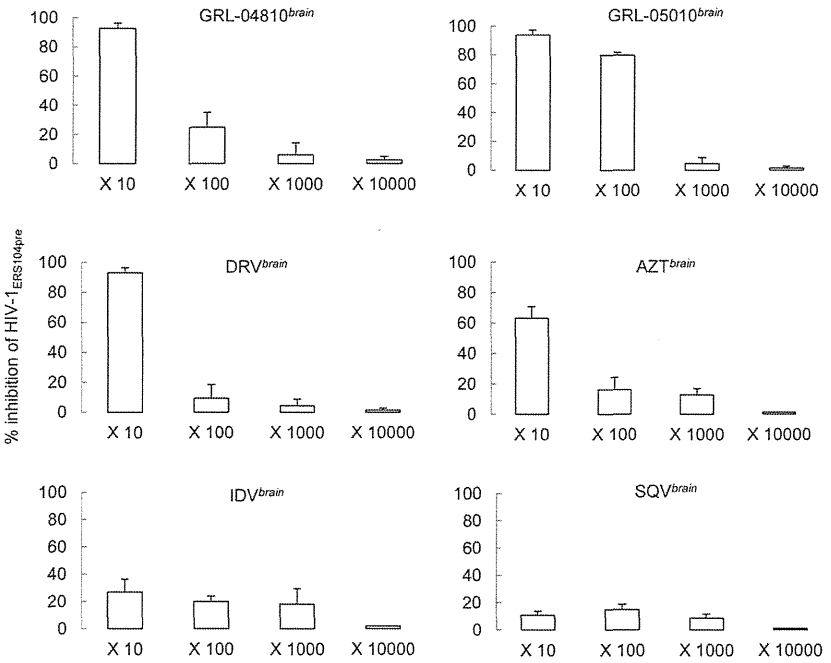

FIG 6 Antiviral activity of GRL-04810^{brain}, GRL-05010^{brain}, DRV^{brain}, AZT^{brain}, IDV^{brain} and SQV^{brain} against HIV-$1_{ERS104pre}$. Compounds recovered from the brain side of the medium in the BBB *in vitro* assay were challenged with HIV-$1_{ERS104pre}$, as indicated, in a p24 assay using PHA-PBMC. Dilution ranges were between 10-fold and 10,000-fold, and the percentage of viral inhibition was used as an endpoint. It is assumed that the greater the percentage of inhibition of HIV-$1_{ERS104pre}$, the greater the concentration of the drug in the brain side medium. Assays were conducted in duplicate, and error bars show standard deviations.

susceptibility assay, virtually the same antiviral profiles of GRL-04810^{brain} and GRL-05010^{brain} were observed (Fig. 6).

Molecular interactions of GRL-04810 and GRL-05010 with wild-type HIV-1 protease. We generated molecular models of the interactions of GRL-04810 and GRL-05010 with wild-type HIV-1 protease. A bird's eye view of GRL-04810 bound to protease is shown in Fig. 7A. The interactions of DRV with HIV-1 protease seen in a crystal structure (Fig. 7B) share key interactions with both GRL-04810 and GRL-05010 as follows. Analysis of the model structure revealed that both oxygen atoms present in the *bis*-THF group of GRL-04810 have polar interactions with the backbone nitrogens of Asp29 and Asp30 in the S2 site of the protease (Fig. 7C). The *O*-methoxy oxygen has a polar interaction with the backbone NH of Asp30′ in the S2′ site of the protease. GRL-04810 maintains polar interactions with Gly27 and Asp25, as well as with Ile50 and Ile50′, through a bridging water molecule. The oxygens in the *bis*-THF group of GRL-05010 also exhibit polar interactions with Asp29 and Asp30 in the S2 site of protease (Fig. 7D). Polar interactions with Gly27, the catalytic Asp25, and the bridging water molecule are also seen for GRL-05010. Even though both GRL-04810 and GRL-05010 form polar interactions with Asp30′ in the S2′ site of the protease, there is a subtle difference due to the different chemical moieties present in the P2′ sites of these inhibitors. The *O*-methoxy oxygen forms a polar contact with the backbone NH of Asp30′, while the NH nitrogen of GRL-05010 forms a polar contact with the backbone carboxyl of Asp30′. The fluoride atoms in the *bis*-THF group of GRL-04810 and GRL-05010 fill the otherwise empty cavity toward the HIV-1 protease flap.

DISCUSSION

DRV is an HIV-1 protease inhibitor which was most recently added to the armamentarium of antiretroviral therapeutics. DRV exerts highly effective activity against a wide spectrum of multidrug-resistant HIV-1 variants including multi-PI-resistant variants and has been shown to resist the emergence of DRV-resistant HIV-1 strains *in vitro* (36, 43) and in the clinical setting (44–46). The mechanisms of the favorable antiretroviral activity and delayed emergence of DRV-resistant strains include the presence of a unique moiety, *bis*-THF, in the P2′ site and DRV's dual action to block HIV-1 protease's enzymatic activity (28, 47) and protease's dimerization (48). However, the penetration of DRV into the cerebrospinal fluid (CSF) is only moderate, with a ratio of DRV concentration in the CSF to that in peripheral blood of 0.6% (49), probably due to the only moderate penetration of DRV through the blood-brain barrier. The addition of fluorine atoms to nucleoside analogs is known to increase lipophilicity and possibly enhance CSF penetration (37, 39). Thus, in the present study, we newly designed, synthesized, and characterized two PIs, GRL-04810 and GRL-05010, which contain a *bis*-THF moiety to which a difluoride group is attached.

GRL-04810 and GRL-05010 suppressed various HIV-1 isolates, including multidrug-resistant clinical HIV-1 isolates with reasonably low EC_{50}s and favorable cytotoxicity profiles although, as in the case of DRV, both PIs failed to efficiently block the replication of APV-resistant strains. To our knowledge, the suppression failure of APV-resistant variants has largely been seen in all of the *bis*-THF-containing PIs thus far published (28, 31–33). The reduced activity of the *bis*-THF-containing PIs to block the replication of APV-resistant variants is likely due to the structural similarity between the *bis*-THF-containing PIs, including GRL-04810, GRL-05010, and DRV.

In the present wild-type HIV-1_{NL4-3} selection experiment with the two PIs, the development of resistance against each compound

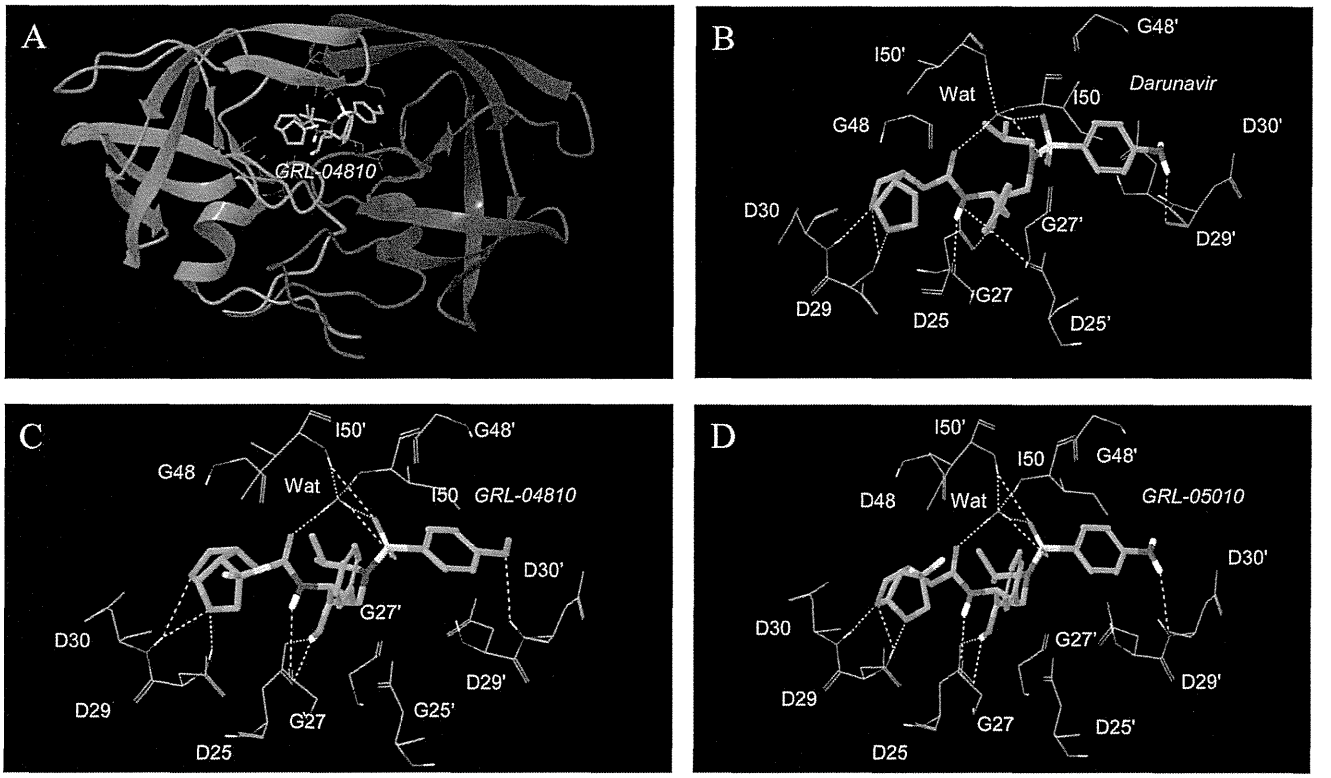

FIG 7 Structural interactions of GRL-04810 and GRL-05010 with HIV-1 protease. A model of GRL-04810 bound to protease is shown (A). GRL-04810 is shown in thick sticks, and residues in the protease active site are shown in wire. The following atom colors are used: carbons in gray, oxygens in red, fluorines in green, nitrogens in blue, and sulfurs in yellow. The polar interactions (yellow dotted lines) of DRV, GRL-04810, and GRL-05010, along with other residues in the active site, are shown in panels B, C, and D, respectively. Nonpolar hydrogens are not shown. Figures were generated using Maestro, version 9.3. (Schrödinger, LLC, New York, NY).

exhibited different patterns from those of the two control PIs, LPV and DRV. In the case of GRL-05010, by passage 10, two PI resistance-associated amino acid substitutions (M46I and I50V) were identified, while HIV-1_{NL4-3} exposed to GRL-04810 acquired three amino acid substitutions, A28S, L33F, and V82I, by passage 20 in 5 of 22 clones examined (Fig. 3). The emergence of the A28S substitution has previously been documented as a resistance-conferring amino acid substitution when HIV-1_{NL4-3} was selected with two *bis*-THF-containing PIs, TMC-126 (35) and GRL-1398 (32), both of which also contain a paramethoxy group in the P2′ site. Intriguingly, when HIV-1_{NL4-3} was selected with GRL-0519, which contains the same paramethoxy group in the P2′ site, the A28S substitution never appeared by up to passage 37 (50). GRL-0519 has *tris*-tetrahydrofuranylurethane (*tris*-THF) as the P2 ligand and the paramethoxy moiety at the P2′ site, suggesting that the presence of *tris*-THF prevented the selection of the A28S substitution. Indeed, to our knowledge, even with long-term administration of DRV, HIV-1 containing the A28S substitution has not been documented in the clinical settings (51). Considering that the selection of HIV-1_{NL4-3} and even a mixture of eight multi-PI-resistant clinical strains with DRV failed to select out the A28S substitution (36) and that only GRL-04810 selection of HIV-1_{NL4-3} resulted in the emergence of the A28S substitution in the present study, the combination of *bis*-THF as the P2 ligand and the paramethoxy moiety at the P2′ site seems to be associated with the emergence of the A28S substitution. As illustrated in Fig. 3, it is of note that the emergence of 2 to 3 amino acid substitutions known to be associated with HIV-1's acquisition of PI resistance in the selection assays with the two novel PIs and no emergence of amino acid substitutions in the selection with DRV may possibly pose a disadvantage for GRL-04810 and GRL-05010 with respect to DRV.

Zidovudine (ZDV) is the only AIDS-associated retrovirus (ARV) agent with demonstrated efficacy in the treatment of HIV-1-associated dementia. Considering that HIV-1 causes CNS diseases ranging from HIV-1-associated neurocognitive disorders (HAND) and the milder, but also serious, presentation, HIV-1-associated minor cognitive/motor disorder (MCMD), to the devastating HIV-1-associated encephalopathy, more effective ARV regimens with agents exerting maximal penetration of the BBB are urgently needed. It is well established that the lipophilicity of a molecule is one of the crucial determinants of the molecule's drug-likeness, including the absorption through the digestive tract, penetration of the target cells, oral bioavailability, and penetration through the BBB (37, 39). The shake flask method represents a reasonable way to determine the partition and distribution coefficients of molecules to be tested. The partition (log *P*) coefficient is an estimate of a compound's overall lipophilicity, which is associated with the compound's solubility, permeability through biological membranes, hepatic clearance, lack of selectivity, and nonspecific toxicity (52). In the present study, the log *P* determination of GRL-04810 gave a higher concentration in the octanol

(lipidic) interface than GRL-05010 and DRV (Table 4). To estimate the actual figures for the ionized form of the drugs (log *D*) Tris-buffered saline (pH 7.4) must be employed. In both assays the values displayed by both GRL-05010 and DRV were within the acceptable range for the optimal lipophilicity of drug candidates (53, 54).

Cell culture-based models have greatly contributed to the understanding of the physiology, pathology, and pharmacology of the blood-brain barrier (41). Indeed, certain *in vitro* BBB models have proven to serve as useful tools that permit the estimation of the apparent penetration of molecules into the CNS. GRL-04810 and GRL-05010 gave reasonably favorable indexes, suggesting potentially favorable penetration ability across the BBB compared to DRV and other anti-HIV-1 drugs examined in the present study, including AZT, IDV, SQV, LPV, and ATV.

A well-characterized *in vitro* BBB cell model can also provide a valuable tool for studying mechanistic aspects of transport as well as biological and pathological processes related to the BBB (42). For any *in vitro* BBB cell model to be employed successfully, it needs to fulfill a number of criteria, such as reproducible permeability of reference compounds, good screening capacity, the display of complex tight junctions, adequate expression of BBB phenotypic transporters, and transcytotic activity. The BBB model employed in the present study complies with all of these parameters and provides an additional advantage as it incorporates a trilayer of cells consisting of astrocytes, pericytes, and brain endothelial cells, thus increasing its anatomical and physiological reliability. Molecules and compounds that reach P_{app} values greater than 20×10^{-6} cm/s are deemed to be favorable in terms of relative penetration across the BBB. Conversely, those that display values between 2×10^{-6} cm/s and 10×10^{-6} cm/s are defined as compounds with low BBB penetration. In the present work, both GRL-05010 and GRL-04810 showed the highest values of P_{app} among the protease inhibitors examined, with values of 47.8×10^{-6} and 61.8×10^{-6} cm/s, respectively (Table 5).

When we asked whether GRL-04810 and GRL-05010 harvested from the brain interface in the BBB model retained antiviral activity, both the recovered GRL-04810 and GRL-05010 (termed GRL-04810^{brain} and GRL-05010^{brain}) significantly more profoundly suppressed the replication of HIV-1_{LAI} and HIV-$1_{ERS104pre}$ than other antiretroviral agents including DRV (Fig. 5 and 6), strongly suggesting that both GRL-04810 and GRL-05010 that crossed into the brain interface in the BBB assay were molecularly intact and exerted robust anti-HIV-1 activity.

The present data suggest that GRL-04810 and GRL-05010 have several advantages: (i) they exert efficient activity against a wide spectrum of drug-resistant HIV-1 variants, presumably due to their interactions with the main chains of the active-site amino acids Asp29 and Asp30, (ii) they have a good lipophilicity profile as expressed by the log *D* values, and (iii) they have apparently favorable penetration across the BBB. However, their oral bioavailability, pharmacokinetics/pharmacodynamics, and volume of distribution, among other parameters, are yet to be determined in further rigorous preclinical and clinical testing.

ACKNOWLEDGMENTS

The present work was supported in part by a grant for global education and a research center aiming at the control of AIDS (Global Center of Excellence supported by Monbu-Kagakusho), the Promotion of AIDS Research from the Ministry of Health, Welfare, and Labor of Japan, a grant to the Cooperative Research Project on Clinical and Epidemiological Studies of Emerging and Re-emerging Infectious Diseases (Renkei Jigyo: number 78, Kumamoto University) of Monbu-Kagakusho (H.M.), the Intramural Research Program of Center for Cancer Research, National Cancer Institute, National Institutes of Health (H.M.), and a grant from the National Institutes of Health (GM53386 to A.K.G.).

Our appreciation also goes to Yasuhiro Koh and Yasushi Tojo for their valuable suggestions during this work.

REFERENCES

1. Coiras M, Lopez-Huertas M, Perez-Olmeda M, Alcami J. 2009. Understanding HIV-1 latency provides clues for the eradication of long-term reservoirs. Nat. Rev. Microbiol. 7:798–812.
2. De Clercq. 2002. New anti-HIV agents and targets. Med. Res. Rev. 22: 531–565.
3. Gorantla S, Poluektova L, Gendelman HE. 2012. Rodent models for HIV-associated neurocognitive disorders. Trends Neurosci. 35:197–208.
4. Lewin SR, Murray J, Solomon A, Wightman F, Cameron PU, Purcell DJ, Zaunders JJ, Grey P, Bloch M, Smith D, Cooper DA, Kelleher AD. 2008. Virological determinants of success after structured treatment interruptions of antiretrovirals in acute HIV-1 infection. J. Acquir. Immune Defic. Syndr. 47:140–147.
5. Siliciano JD, Siliciano RF. 2004. A long-term latent reservoir for HIV-1: discovery and clinical implications. J. Antimicrob. Chemother. 54:6–9.
6. Simon V, Ho DD. 2003. HIV-1 dynamics in vivo: implications for therapy. Nat. Rev. Microbiol. 1:181–190.
7. Carr. 2003. Toxicity of antiretroviral therapy and implications for drug development. Nat. Rev. Drug Discov. 2:624–634.
8. Fumero E, Podzamczer D. 2003. New patterns of HIV-1 resistance during HAART. Clin. Microbiol. Infect. 9:1077–1084.
9. Grabar S, Abraham B, Mahamat A, Del Giudice P, Rosenthal E, Costagliola D. 2006. Differential impact of combination antiretroviral therapy in preventing Kaposi's sarcoma with and without visceral involvement. J. Clin. Oncol. 24:3408–3414.
10. Hirsch HH, Kaufmann G, Sendi P, Battegay M. 2004. Immune reconstitution in HIV-infected patients. Clin. Infect. Dis. 38:1159–1166.
11. Little SJ, Holte S, Routy JP, Daar ES, Markowitz M, Collier AC, Koup RA, Mellors JW, Connick E, Conway B, Kilby M, Wang L, Whitcomb JM, Hellmann NS, Richman DD. 2002. Antiretroviral-drug resistance among patients recently infected with HIV. N. Engl. J. Med. 347:385–394.
12. Enting RH, Hoetelmans R, Lange JM, Burger DM, Beijnen JH, Portegies P. 1998. Antiretroviral drugs and the central nervous system. AIDS 12:1941–1955.
13. Kramer-Hammerle S, Rothenaigner I, Wolff H, Bell JE, Brack-Werner R. 2005. Cells of the central nervous system as targets and reservoirs of the human immunodeficiency virus. Virus Res. 111:194–213.
14. McArthur JC, Brew BJ, Nath A. 2005. Neurological complications of HIV infection. Lancet Neurol. 4:543–555.
15. Langford D, Marquie-Beck J, de Almeida S, Lazzaretto D, Letendre S, Grant I, McCutchan JA, Masliah E, Ellis RJ. 2006. Relationship of antiretroviral treatment to postmortem brain tissue viral load in human immunodeficiency virus-infected patients. J. Neurovirol. 12:100–107.
16. Nath A, Sacktor N. 2006. Influence of highly active antiretroviral therapy on persistence of HIV in the central nervous system. Curr. Opin. Neurol. 19:358–361.
17. Potter MC, Figuera-Losada M, Rojas C, Slusher BS. 2013. Targeting the glutamatergic system for the treatment of HIV-associated neurocognitive disorders. J. Neuroimmune Pharmacol. 8:594–607.
18. Sacktor. 2002. The epidemiology of human immunodeficiency virus-associated neurological disease in the era of highly active antiretroviral therapy. J. Neurovirol. 8:115–121.
19. Tan IL, McArthur JC. 2012. HIV-associated neurological disorders: a guide to pharmacotherapy. CNS Drugs 26:123–134.
20. Smit TK, Brew BJ, Tourtellotte W, Morgello S, Gelman BB, Saksena NK. 2004. Independent evolution of human immunodeficiency virus (HIV) drug resistance mutations in diverse areas of the brain in HIV-infected patients, with and without dementia, on antiretroviral treatment. J. Virol. 78:10133–10148.
21. Gisolf EH, Van Praaq R, Jurriaans S, Portegies P, Goudsmit J, Danner SA, Lange JM, Prins JM. 2000. Increasing cerebrospinal fluid chemokine concentrations despite undetectable cerebrospinal fluid HIV RNA in

HIV-1-infected patients receiving antiretroviral therapy. J. Acquir. Immune Defic. Syndr. 25:426–433.
22. Lipton SA, Brenneman Silverstein DFS, Masliah E, Mucke L. 1995. gp120 and neurotoxicity in vivo. Trends Pharmacol. Sci. 16:122.
23. Neuenburg JK, Brodt HR, Herndier BG, Bickel M, Bacchetti P, Price RW, Grant RM, Schlote W. 2002. HIV-related neuropathology, 1985 to 1999: rising prevalence of HIV encephalopathy in the era of highly active antiretroviral therapy. J. Acquir. Immune Defic. Syndr. 31:171–177.
24. Schrager LK, D'Souza MP. 1998. Cellular and anatomical reservoirs of HIV-1 in patients receiving potent antiretroviral combination therapy. JAMA 280:67–71.
25. Kaul M, Garden G, Lipton SA. 2001. Pathways to neuronal injury and apoptosis in HIV-associated dementia. Nature 410:988–994.
26. Ghosh AK, Krishnan K, Walters DE, Cho W, Cho H, Koo Y, Trevino J, Holland L, Buthod J. 1998. Potent HIV protease inhibitors incorporating high-affinity P2-ligands and (*R*)-(hydroxyethylamino)sulfonamide isostere. Bioorg. Med. Chem. Lett. 8:687–690.
27. Ghosh AK, Cho W, Walters DE, Krishnan K, Hussain KA, Koo Y, Cho H, Rudall C, Holland L, Buthod J. 1998. Structure based design: novel spirocyclic ethers as nonpeptidal P2-ligands for HIV protease inhibitors. Bioorg. Med. Chem. Lett. 8:979–982.
28. Koh Y, Nakata H, Maeda K, Ogata H, Bilcer G, Devasamudram T, Kincaid JF, Boross P, Wang YF, Tie Y, Volarath P, Gaddis L, Harrison RW, Weber IT, Ghosh AK, Mitsuya H. 2003. Novel *bis*-tetrahydrofuranylurethane-containing nonpeptidic protease inhibitor (PI) UIC-94017 (TMC114) with potent activity against multi-PI-resistant human immunodeficiency virus in vitro. Antimicrob. Agents Chemother. 47:3123–3129.
29. Shirasaka T, Chokekijchai S, Yamada A, Gosselin G, Imbach JL, Mitsuya H. 1995. Comparative analysis of anti-human immunodeficiency virus type 1 activities of dideoxynucleoside analogs in resting and activated peripheral blood mononuclear cells. Antimicrob. Agents Chemother. 39:2555–2559.
30. Ghosh AK, Leshchenko S, Noetzel M. 2004. Stereoselective photochemical 1,3-dioxolane addition to 5-alkoxymethyl-2(5*H*)-furanone: synthesis of *bis*-tetrahydrofuranyl ligand for HIV protease inhibitor UIC-94017 (TMC-114). J. Org. Chem. 69:7822–7829.
31. Amano M, Koh Y, Das D, Li J, Leschenko S, Wang YF, Boross PI, Weber IT, Ghosh AK, Mitsuya H. 2007. A novel *bis*-tetrahydrofuranylurethane-containing nonpeptidic protease inhibitor (PI), GRL-98065, is potent against multiple-PI-resistant human immunodeficiency virus *in vitro*. Antimicrob. Agents Chemother. 51:2143–2155.
32. Ide K, Aoki M, Amano M, Koh Y, Yedidi RS, Das D, Leschenko S, Chapsal B, Ghosh AK, Mitsuya H. 2011. Novel HIV-1 protease inhibitors (PIs) containing a bicyclic P2 functional moiety, tetrahydropyranotetrahydrofuran, that are potent against multi-PI-resistant HIV-1 variants. Antimicrob. Agents Chemother. 55:1717–1727.
33. Tojo Y, Koh Y, Amano M, Aoki M, Das D, Kulkarni S, Anderson DD, Ghosh AK, Mitsuya H. 2010. Novel protease inhibitors (PIs) containing macrocyclic components and 3(*R*),3a(*S*),6a(*R*)-*bis*-tetrahydrofuranylurethane that are potent against multi-PI-resistant HIV-1 variants *in vitro*. Antimicrob. Agents Chemother. 54:3460–3470.
34. Nakagawa S, Deli MA, Kawaguchi H, Shimizudani T, Shimono T, Kittel A, Tanaka K, Niwa M. 2009. A new blood-brain barrier model using primary rat brain endothelial cells, pericytes and astrocytes. Neurochem. Int. 54:253–263.
35. Yoshimura K, Kato R, Kavlick MF, Nguyen A, Maroun V, Maeda K, Hussain KA, Ghosh AK, Gulnik SV, Erickson JW, Mitsuya H. 2002. A potent human immunodeficiency virus type 1 protease inhibitor, UIC-94003 (TMC-126), and selection of a novel (A28S) mutation in the protease active site. J. Virol. 76:1349–1358.
36. Koh Y, Amano M, Towata T, Danish M, Leshchenko-Yashchuk S, Das D, Nakayama M, Tojo Y, Ghosh AK, Mitsuya H. 2010. In vitro selection of highly darunavir-resistant and replication-competent HIV-1 variants by using a mixture of clinical HIV-1 isolates resistant to multiple conventional protease inhibitors. J. Virol. 84:11961–11969.
37. Bright TV, Dalton F, Elder VL, Murphy CD, O'Connor NK, Sandford G. 2013. A convenient medical-microbial method for developing fluorinated pharmaceuticals. Org. Biomol. Chem. 11:1135–1142.
38. Karppi J, Akerman S, Akerman K, Sundell A, Nyyssonen K, Penttila I. 2007. Adsorption of drugs onto apH responsive poly(*N,N* dimethyl aminoethyl methacrylate) grafted anion-exchange membrane in vitro. Int. J. Pharm. 338:7–14.
39. Liu P, Sharon A, Chu CK. 2008. Fluorinated nucleosides: synthesis and biological implication. J. Fluor. Chem. 129:743–766.
40. Rak J, Dejlová B, Lampová H, Kaplánek R, Matějíček P, Cígler P, Král V. 2013. On the solubility and lipophilicity of metallacarborane pharmacophores. Mol. Pharm. 10:1751–1759.
41. Nakagawa S, Deli MA, Nakao S, Honda M, Hayashi K, Nakaoke R, Kataoka Y, Niwa M. 2007. Pericytes from brain microvessels strengthen the barrier integrity in primary cultures of rat brain endothelial cells. Cell. Mol. Neurobiol. 27:687–694.
42. Cecchelli R, Berezowski V, Lundquist S, Culot M, Renftel M, Dehouck MP, Fenart L. 2007. Modelling of the blood brain barrier in drug discovery and development. Nat. Rev. Drug Discov. 6:650–661.
43. de Bethune MP, Hertogs K. 2006. Screening and selecting for optimized antiretroviral drugs: rising to the challenge of drug resistance. Curr. Med. Res. Opin. 22:2603–2612.
44. Geretti AM, Arribas J, Lathouwers E, Foster GM, Yakoob R, Kinloch S, Hill A, van Delft Y, Moecklinghoff C. 2013. Dynamics of cellular HIV-1 DNA levels over 144 weeks of darunavir/ritonavir monotherapy versus triple therapy in the MONET trial. HIV Clin. Trials 14:45–50.
45. Orkin C, DeJesus E, Khanlou H, Stoehr A, Supparatpinyo K, Lathouwers E, Lefebvre E, Opsomer M, Van de Casteele T, Tomaka F. 2013. Final 192-week efficacy and safety of once-daily darunavir/ritonavir compared to lopinavir/ritonavir in HIV-1-infected treatment-naive patients in the ARTEMIS trial. HIV Med. 14:49–59.
46. Banhegyi D, Katlama C, da Cunha CA, Schneider S, Rachlis A, Workman C, De Meyer S, Vandevoorde A, Van De Casteele T, Tomaka F. 2012. Week 96 efficacy, virology and safety of darunavir/r versus lopinavir/r in treatment-experienced patients in TITAN. Curr. HIV Res. 10:171–181.
47. Ghosh AK, Xu CX, Rao KV, Baldridge A, Agniswamy J, Wang YF, Weber IT, Aoki M, Miguel SG, Amano M, Mitsuya H. 2010. Probing multidrug-resistance and protein-ligand interactions with oxatricyclic designed ligands in HIV-1 protease inhibitors. ChemMedChem 5:1850–1854.
48. Koh Y, Matsumi S, Das D, Amano M, Davis DA, Leschenko S, Baldridge A, Shioda T, Yarchoan R, Ghosh AK, Mitsuya H. 2007. Potent inhibition of HIV-1 replication by novel non-peptidyl small molecule inhibitors of protease dimerization. J. Biol. Chem. 282:28709–28720.
49. Calcagno A, Yilmaz A, Cusato J, Simiele M, Bertucci R, Siccardi M, Marinaro L, D'Avolio A, Di Perri G, Bonora S. 2012. Determinants of darunavir cerebrospinal fluid concentrations: impact of once-daily dosing and pharmacogenetics. AIDS 26:1529–1533.
50. Amano M, Tojo Y, Salcedo-Gomez PM, Campbell JR, Das D, Aoki M, Xu CX, Rao KV, Ghosh AK, Mitsuya H. 2013. GRL-0519, a novel oxatricyclic ligand-containing nonpeptidic HIV-1 protease inhibitor (PI), potently suppresses replication of a wide spectrum of multi-PI-resistant variants *in vitro*. Antimicrob. Agents Chemother. 57:2036–2046.
51. Mitsuya Y, Varghese V, Wang C, Liu TF, Holmes SP, Jayakumar P, Gharizadeh B, Ronaghi M, Klein D, Fessel WJ, Shafer RW. 2008. Minority human immunodeficiency virus type 1 variants in antiretroviral-naive persons with reverse transcriptase codon 215 revertant mutations. J. Virol. 82:10747–10755.
52. Hughes JD, Blagg J, Price DA, Bailey S, Decrescenzo GA, Devraj RV, Ellsworth E, Fobian YM, Gibbs ME, Gilles RW, Greene N, Huang E, Krieger-Burke T, Loesel J, Wager T, Whiteley L, Zhang Y. 2008. Physiochemical drug properties associated with in vivo toxicological outcomes. Bioorg. Med. Chem. Lett. 18:4872–4875.
53. Ryckmans T, Edwards MP, Horne VA, Correia AM, Owen DR, Thompson LR, Tran I, Tutt MF, Young T. 2009. Rapid assessment of a novel series of selective CB_2 agonists using parallel synthesis protocols: a lipophilic efficiency (LipE) analysis. Bioorg. Med. Chem. Lett. 19:4406–4409.
54. Waring MJ. 2009. Defining optimum lipophilicity and molecular weight ranges for drug candidates—molecular weight dependent lower log *D* limits based on permeability. Bioorg. Med. Chem. Lett. 19:2844–2851.
55. Organisation for Economic Cooperation and Development. 1995. OECD guidelines for the testing of chemicals, section 1: physical-chemical properties. Test no. 107. Organisation for Economic Cooperation and Development, Paris, France. doi:10.1787/20745753.

AAC
Journals.ASM.org

Evaluation of Combinations of 4′-Ethynyl-2-Fluoro-2′-Deoxyadenosine with Clinically Used Antiretroviral Drugs

Atsuko Hachiya,[a,b]* Aaron B. Reeve,[c] Bruno Marchand,[a] Eleftherios Michailidis,[a] Yee Tsuey Ong,[a] Karen A. Kirby,[a] Maxwell D. Leslie,[a] Shinichi Oka,[b] Eiichi N. Kodama,[d] Lisa C. Rohan,[e,f] Hiroaki Mitsuya,[g,h] Michael A. Parniak,[c] Stefan G. Sarafianos[a,i]

Christopher Bond Life Sciences Center, Department of Molecular Microbiology and Immunology, University of Missouri School of Medicine, Columbia, Missouri, USA[a]; AIDS Clinical Center, National Center for Global Health and Medicine, Tokyo, Japan[b]; Department of Microbiology and Molecular Genetics, University of Pittsburgh, Pittsburgh, Pennsylvania, USA[c]; Division of Emerging Infectious Diseases, Tohoku University, Tohoku Medical Megabank Organization, Miyagi, Japan[d]; Magee-Womens Research Institute[e] and Department of Pharmaceutical Sciences, School of Pharmacy,[f] University of Pittsburgh, Pittsburgh, Pennsylvania, USA; Department of Hematology and Infectious Diseases, Kumamoto University, Kumamoto, Japan[g]; Experimental Retrovirology Section, HIV/AIDS Malignancy Branch, National Institutes of Health, Bethesda, Maryland, USA[h]; Department of Biochemistry, University of Missouri, Columbia, Missouri, USA[i]

Drug combination studies of 4′-ethynyl-2-fluoro-2′-deoxyadenosine (EFdA) with FDA-approved drugs were evaluated by two different methods, MacSynergy II and CalcuSyn. Most of the combinations, including the combination of the two adenosine analogs EFdA and tenofovir, were essentially additive, without substantial antagonism or synergism. The combination of EFdA and rilpivirine showed apparent synergism. These studies provide information that may be useful for the design of EFdA combination regimens for initial and salvage therapy assessment.

Combination antiretroviral therapies provide durable viral suppression and constitute the standard of care for HIV infection (http://www.aidsinfo.nih.gov/guidelines/) (1). For example, the combination of tenofovir disoproxil fumarate (TDF) and emtricitabine (FTC) (Truvada) is one of the preferred regimens for treatment of HIV-1 infection (2, 3). *In vitro* studies have shown that tenofovir (TFV) and FTC have synergistic antiretroviral activity (4, 5).

The investigational nucleoside reverse transcriptase inhibitor (NRTI), 4′-ethynyl-2-fluoro-2′-deoxyadenosine (EFdA) is presently under preclinical evaluation. Unlike other NRTIs used in the treatment of HIV infection, EFdA retains the 3′-hydroxyl moiety. It also contains a 2-fluoro group on the adenine base and a 4′-ethynyl group on the deoxyribose ring. Although EFdA is an adenosine analog, its activation is initiated by phosphorylation by 2′-deoxycytidine kinase (dCK), and the drug is highly resistant to degradation by adenosine deaminase (ADA) (6). EFdA shows exceptional antiretroviral activity *in vitro* (6–8) and *in vivo* (9, 10) as well as a favorable cross-resistance profile with current reverse transcriptase inhibitors (RTIs) used in the clinic.

Studies on potential interactions between EFdA and other antiretroviral drugs can provide information that could be useful in the development of combinatorial therapeutic strategies. The present study evaluates anti-HIV efficacy in combinations of EFdA with representative FDA-approved RTIs *in vitro*.

We first determined the antiviral potencies of five NRTIs (zidovudine [AZT], lamivudine [3TC], FTC, TDF, and EFdA) and three nonnucleoside RTIs (NNRTIs; efavirenz [EFV], etravirine [ETR], and rilpivirine [RPV]) against HIV-1_{NL4-3} in order to obtain an optimal range of drug concentrations for use in combination assay analyses. As previously demonstrated (6, 7), EFdA inhibited HIV-1 replication several orders of magnitude more efficiently than other currently approved NRTIs (Table 1). In the same cell-based assays, we evaluated antiretroviral activity of EFdA in combination with the FDA-approved RTIs. To obtain more comprehensive evaluations of drug combinations and to reduce analysis bias, we use two algorithms provided by the software packages MacSynergy II (version 1.0; Ann Arbor, MI) and CalcuSyn (Biosoft, Ferguson, MO), which are based on the Bliss independence model (11, 12) and the median effect principle (13), respectively. Quantitative differences in data analyses by the two algorithms used by the MacSynergy II and CalcuSyn programs are not uncommon (14). In the present work, drug interactions were considered significant only if detected by both computational approaches.

TABLE 1 Antiviral activity of HIV-1 inhibitors

Compound class and name	EC_{50} (nM) for anti-HIV-1 activity[a]
NRTI	
AZT	180 ± 60
3TC	1,210 ± 240
FTC	370 ± 70
TDF	14 ± 2
EFdA	3 ± 1
NNRTI	
EFV	1.6 ± 0.4
ETR	1 ± 0.1
RPV	0.4 ± 0.1

[a] EC_{50}, 50% effective concentration. Values were determined using the TZM-bl cell line obtained from the NIH AIDS Research and Reference Reagent Program. All assays were conducted in triplicates. The data shown are mean values ± standard deviations obtained from the results of at least three independent experiments.

Received 25 February 2013 Returned for modification 6 April 2013
Accepted 15 June 2013
Published ahead of print 24 June 2013
Address correspondence to Stefan G. Sarafianos, sarafianoss@missouri.edu.
* Present address: Atsuko Hachiya, Clinical Research Center, Department of Infectious Diseases and Immunology, National Hospital Organization Nagoya Medical Center, Nagoya, Japan.
A.H. and A.B.R. contributed equally to this article.

doi:10.1128/AAC.00283-13

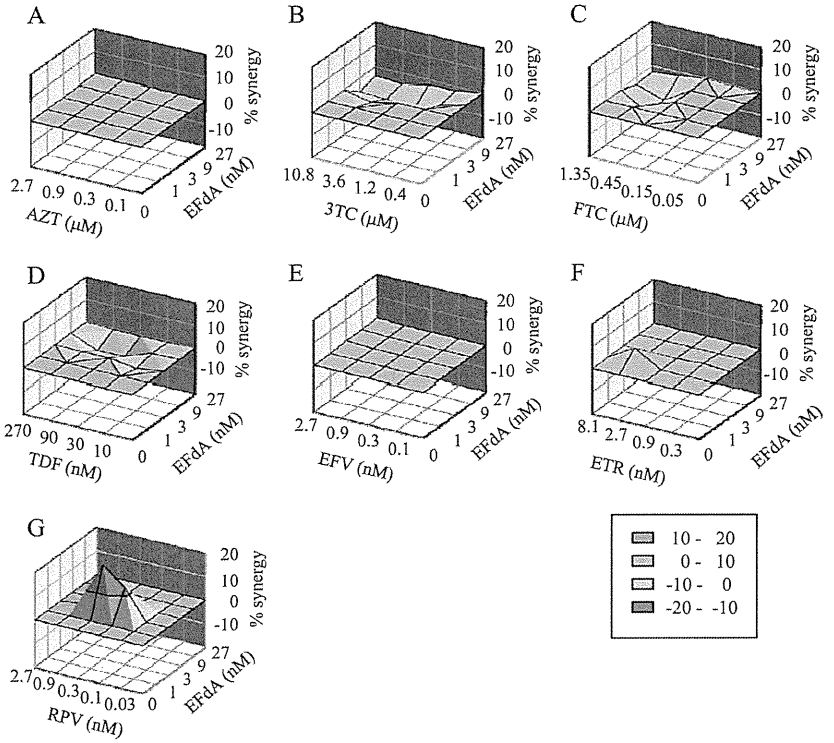

FIG 1 Effects of EFdA in combination with other anti-HIV-1 agents. The calculated additive surface, which represents the predicted additive interactions, is then subtracted from the experimental surface to reveal regions of greater-than-expected interactions (synergy). A resulting surface appearing as a horizontal plane at 0% inhibition above the calculated additive surface suggests that the interactions are merely additive. Peaks of statistically significant synergy (positive value) or antagonism (negative value) that deviate significantly from the expected additive drug interactions derived from 95% confidence interval data are shown in the different plots of the interaction between EFdA and other anti-HIV-1 agents in the cell-based assay, as follows: AZT (A), 3TC (B), FTC (C), TDF (D), EFV (E), ETR (F), and RPV (G). Units of $\mu M^2\%$ are analogous to the units for area under a dose-response curve in the two-dimensional situation.

Most drugs tested, including the adenosine analog TDF, showed little or no drug interactions in combination with EFdA (Fig. 1 and Table 2). Data analysis with CalcuSyn suggested that the combinations of both EFdA and 3TC (EFdA-3TC) and EFdA-FTC are moderately antagonistic (Fig. 1 and Table 2). Using MacSynergy, the EFdA-3TC combination was assessed as minor antagonism, whereas the EFdA-FTC combination was considered additive; however, its value (-23.4 $\mu M^2\%$) was very close to minor antagonism (-25 $\mu M^2\%$). The observed borderline antagonism may arise from competition at the first and rate-limiting

TABLE 2 Interactions of drug combinations for inhibition of HIV-1 virus or RT enzyme

Drug class and EFdA combination	Target	MacSynergy analysis		CalcuSyn analysis		
		Synergy/antagonism ($\mu M^2\%$)[a]	Predicted interaction	CI[b]	Predicted interaction	Proposed interaction[c]
NRTI						
AZT	Virus	0/0	Additive	1.18	Additive	Neutral
TDF	Virus	0/−12.8	Additive	1.36	Moderate antagonism	Neutral
3TC	Virus	0/−39.5	Minor antagonism	1.23	Moderate antagonism	Possible antagonism
FTC	Virus	0/−23.4	Additive	1.25	Moderate antagonism	Neutral
NNRTI						
EFV	Virus	1.9/0	Additive	0.9	Additive	Neutral
ETR	Virus	7.8/0	Additive	1.05	Additive	Neutral
RPV	Virus	41.0/−0.04	Minor synergy	0.64	Synergy	Synergy
RPV	Enzyme	34.1/0	Minor synergy	0.56	Synergy	Synergy

[a] The volume of the peaks in the difference plots at the 95% confidence level, which corresponds to the area under a dose-response curve and is considered to provide a quantitative measure of possible drug interactions. MacSynergy II defines $\mu M^2\%$ values as follows: 25 to 50, minor synergy; 50 to 100, moderate synergy; >100, strong synergy. The corresponding negative value ranges reflect minor, moderate, and strong antagonism, respectively. Values between 25 and -25 $\mu M^2\%$ are considered insignificant.

[b] CI, combination Index. CalcuSyn defines CI values as follows: 0.1 to 0.3, strong synergy; 0.3 to 0.7, synergy; 0.7 to 0.85, moderate synergy; 0.85 to 1.2, additive; 1.2 to 1.45, moderate antagonism; 1.45 to 3.3, antagonism; 3.3 to 10, strong antagonism.

[c] Proposed interaction is assessed on the basis of the predictions by the two computational methods. Neutral, a lack of drug interaction in the combination (additivity).

TABLE 3 Antiviral and prophylactic activity of EFdA, RPV, and EFdA-RPV combinations

Activity type (pretreatment) and virus	Drug treatment[a]	EC_{50} (nM)[b]	CI_{50}[c]
Antiviral activity			
Wild type	EFdA	0.9 ± 0.2	
	RPV	0.7 ± 0.1	
	EFdA-RPV	0.4 ± 0.2	0.55
M184V	EFdA	15 ± 3	
	RPV	0.6 ± 0.2	
	EFdA-RPV	0.7 ± 0.1	0.5
L100I/K103N	EFdA	1 ± 0.5	
	RPV	10 ± 2	
	EFdA-RPV	9 ± 2	0.45
Prophylaxis (2-h preincubation)			
Wild type	EFdA	11 ± 5	
	RPV	18 ± 4	
	EFdA-RPV	5 ± 2	0.75
M184V	EFdA	97 ± 22	
	RPV	8 ± 2	
	EFdA-RPV	10 ± 3	1
L100I/K103N	EFdA	12 ± 3	
	RPV	175 ± 42	
	EFdA-RPV	9 ± 2	0.6
Prophylaxis (18-h preincubation)			
Wild type	EFdA	3 ± 1	
	RPV	21 ± 4	
	EFdA-RPV	4 ± 1	0.9
M184V	EFdA	53 ± 13	
	RPV	14 ± 4	
	EFdA-RPV	13 ± 40	0.6
L100I/K103N	EFdA	6 ± 1	
	RPV	250 ± 25	
	EFdA-RPV	5 ± 2	0.75

[a] EFdA and RPV were combined at a 1:1 ratio.

[b] EC_{50}, 50% effective concentration. The data shown are mean values ± standard deviations obtained from the results of at least three independent experiments using P4R5-MAGI cells (32).

[c] CI_{50} is the calculated combination index at a 50% inhibitory concentration.

phosphorylation step as EFdA, 3TC, and FTC are all initially activated by 2′-deoxycytidine kinase (6, 15, 16). Small differences in the effect of 3TC versus FTC may arise from the longer half-life of FTC. In contrast, the combination of EFdA-RPV demonstrated apparently significant synergy, as assessed by the two different methods (41 μM^2% in MacSynergy and 0.64 combination index [CI] in CalcuSyn). To confirm the synergy of HIV-1 inhibition by EFdA-RPV, we further evaluated this combination in the enzymatic assay for reverse transcriptase. Primer extension assays (7, 17) were performed with Quant-iT PicoGreen reagent (Invitrogen, Carlsbad, CA) (18). As shown in Table 2, the combination of EFdA with RPV provided synergistic effects on inhibition of reverse transcription.

We further compared the antiretroviral activity of various concentrations of EFdA alone, RPV alone, and a 1:1 molar combination of EFdA and RPV against wild-type virus and two HIV-1 mutants with reverse transcriptase (RT) mutations M184V and L100I/K103N. To evaluate the ability of the drugs to establish a barrier to subsequent infection in the absence of exogenous drug, cells were pretreated with various concentrations of each drug alone or in combination, followed by removal of exogenous drug and inoculation with HIV-1. These conditions assess intracellular persistence of drug following exogenous drug clearance, which is dependent on the intracellular half-life of the test drugs. The EFdA-RPV combination provided additive to synergistic inhibition of wild-type HIV-1 and both mutant strains (Table 3). The protective effect established by EFdA pretreatment is likely the result of EFdA resistance to degradation by adenosine deaminase (ADA) (6), consistent with a longer intracellular half-life (19). Hence, our data suggest that EFdA could be a strong candidate for use in preexposure prophylaxis, an approach in which TDF has shown efficacy in clinical studies (20, 21).

Finally, we evaluated the ability of EFdA-RPV pretreatment to protect MT-2 lymphoblastoid cells from infection by a mixed virus population consisting of six HIV-1 strains: the wild type; the mutants K65R, Y181C, M184V, and D67N/K70R/T215F/K219Q (thymidine analogue mutations [TAMs]); and L100I/K103N. Cells were exposed to appropriate drugs for 16 h, and then exogenous drug was removed (Fig. 2). The breakthrough virus population harvested from cells not exposed to drug contained all six input viruses, plus some recombinant strains (Fig. 2B). Rapid virus breakthrough was evident in cells pretreated with RPV alone, and the only virus detected in the RPV-breakthrough population was the NNRTI-resistant L100I/K103N (100%). In contrast, breakthrough in cells pretreated with EFdA alone was significantly delayed. The EFdA-breakthrough population contained a mixture of the NRTI-resistant M184V mutant (54%) and TAMs (32%), plus some recombinant strains consisting of M184V plus one or more TAMs. No breakthrough was noted in cells pretreated with the EFdA-RPV combination, suggesting an enhanced protective effect of the drug combination compared to either drug alone.

Synergistic interactions between NRTIs and NNRTIs have been previously reported in both viral (5, 22–24) and enzymatic assays (5, 25–31). NNRTIs may act synergistically with NRTIs by

A

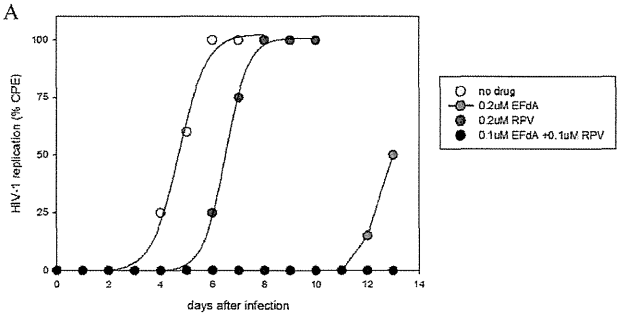

B

Virus	% of breakthrough virus			
	No drug	0.2 μM RPV	0.2 μM EFdA	Combination
Wild-type	20	0	0	-
K65R	15	0	0	-
M184V	3.5	0	54	-
TAMs	6	0	32	-
Y181C	17	0	0	-
L100I/K103N	28	100	0	-
Recombinant	10.5	0	14	-

FIG 2 HIV-1 breakthrough in cells pretreated with EFdA, RPV, or a combination of EFdA and RPV. (A) MT-2 cells were incubated with the indicated concentrations of drug for 18 h and then extensively washed to remove exogenous drug. The washed cells were infected with a mixture of six virus strains (the wild type and five drug-resistant variants). Cells were examined daily for HIV-induced cytopathic effects. (B) Genotypic composition of breakthrough virus is shown. At least 20 clones from each breakthrough virus were sequenced. EFdA (0.1 μM) and RPV (0.1 μM) were used in combination. No virus breakthrough was noted in cells pretreated with the EFdA-RPV combination. TAMs (thymidine analog resistance mutations) included the D67N, K70R, T210F, and T219Q RT mutations. Recombinant virus possessed mutations derived from at least two of the input virus strains.

suppressing the phosphorolytic unblocking of NRTI-terminated primers, possibly by stabilizing the primer terminus at a posttranslocation position, where it cannot undergo phosphorolytic removal (5, 26, 27, 29). The mechanism for the apparent synergistic activity of the EFdA-RPV combination is under investigation.

In conclusion, EFdA in combination with RPV may provide a beneficial interaction against replication of drug-sensitive and certain RTI-resistant HIV-1 strains. The results of the present study indicate that EFdA may act as promising component of future antiretroviral therapies.

ACKNOWLEDGMENTS

This work was supported by a grant for the Bilateral International Collaborative R&D Program from the Korean Food and Drug Administration and the Ministry of Knowledge and Economy (S.G.S.), by National Institutes of Health (NIH) research grants AI076119-S1, AI076119-02S1, AI100890, AI099284, AI094715, AI076119, AI074389, and GM103368 to S.G.S. and AI079801 to M.A.P., and by a Grant-in-Aid for the research on HIV/AIDS (H22-AIDS-001) from the Ministry of Health, Labor, and Welfare of Japan (S.O.). B.M. was the recipient of an amfAR Mathilde Krim Fellowship and a Canadian Institutes of Health Research (CIHR) Fellowship. We acknowledge the Yamasa Corporation for providing EFdA for this study.

H.M. and E.N.K. are coinventors of EFdA.

A.H. carried out the cell-based drug combination assays and wrote the manuscript. A.B.R. carried out the viral breakthrough experiments and studies with drug-resistant HIV and wrote portions of the manuscript. B.M., E.M., Y.T.O., K.A.K., and M.D.L. carried out the biochemical assays. S.G.S., M.A.P., S.O., and H.M. contributed to the design of the study, and S.G.S., L.C.R., E.N.K., and M.A.P. edited the manuscript. All authors read this paper and approved the final manuscript.

REFERENCES

1. Thompson MA, Aberg JA, Hoy JF, Telenti A, Benson C, Cahn P, Eron JJ, Gunthard HF, Hammer SM, Reiss P, Richman DD, Rizzardini G, Thomas DL, Jacobsen DM, Volberding PA. 2012. Antiretroviral treatment of adult HIV infection: 2012 recommendations of the International Antiviral Society-USA panel. JAMA 308:387–402.
2. James JS. 2004. FDA approves two combination pills, Epzicom and Truvada; comment on commercial race to once-a-day nucleosides. AIDS Treat News 403:6. http://www.aidsnews.org/2004/08/epzicom-truvada.html.
3. Killingley B, Pozniak A. 2007. The first once-daily single-tablet regimen for the treatment of HIV-infected patients. Drugs Today 43:427–442.
4. Borroto-Esoda K, Vela JE, Myrick F, Ray AS, Miller MD. 2006. In vitro evaluation of the anti-HIV activity and metabolic interactions of tenofovir and emtricitabine. Antivir. Ther. 11:377–384.
5. Feng JY, Ly JK, Myrick F, Goodman D, White KL, Svarovskaia ES, Borroto-Esoda K, Miller MD. 2009. The triple combination of tenofovir, emtricitabine and efavirenz shows synergistic anti-HIV-1 activity in vitro: a mechanism of action study. Retrovirology 6:44. doi:10.1186/1742-4690-6-44.
6. Kawamoto A, Kodama E, Sarafianos SG, Sakagami Y, Kohgo S, Kitano K, Ashida N, Iwai Y, Hayakawa H, Nakata H, Mitsuya H, Arnold E, Matsuoka M. 2008. 2′-Deoxy-4′-C-ethynyl-2-halo-adenosines active against drug-resistant human immunodeficiency virus type 1 variants. Int. J. Biochem. Cell Biol. 40:2410–2420.
7. Michailidis E, Marchand B, Kodama EN, Singh K, Matsuoka M, Kirby KA, Ryan EM, Sawani AM, Nagy E, Ashida N, Mitsuya H, Parniak MA, Sarafianos SG. 2009. Mechanism of inhibition of HIV-1 reverse transcriptase by 4′-ethynyl-2-fluoro-2′-deoxyadenosine triphosphate, a translocation-defective reverse transcriptase inhibitor. J. Biol. Chem. 284:35681–35691.
8. Kirby KA, Singh K, Michailidis E, Marchand B, Kodama EN, Ashida N, Mitsuya H, Parniak MA, Sarafianos SG. 2011. The sugar ring conformation of 4′-ethynyl-2-fluoro-2′-deoxyadenosine and its recognition by the polymerase active site of HIV reverse transcriptase. Cell Mol. Biol. 57:40–46.
9. Murphey-Corb M, Rajakumar P, Michael H, Nyaundi J, Didier PJ, Reeve AB, Mitsuya H, Sarafianos SG, Parniak MA. 2012. Response of simian immunodeficiency virus to the novel nucleoside reverse transcriptase inhibitor 4′-ethynyl-2-fluoro-2′-deoxyadenosine in vitro and in vivo. Antimicrob. Agents Chemother. 56:4707–4712.
10. Hattori S, Ide K, Nakata H, Harada H, Suzu S, Ashida N, Kohgo S, Hayakawa H, Mitsuya H, Okada S. 2009. Potent activity of a nucleoside reverse transcriptase inhibitor, 4′-ethynyl-2-fluoro-2′-deoxyadenosine, against human immunodeficiency virus type 1 infection in a model using human peripheral blood mononuclear cell-transplanted NOD/SCID Janus kinase 3 knockout mice. Antimicrob. Agents Chemother. 53:3887–3893.
11. Prichard MN, Prichard LE, Shipman C, Jr. 1993. Strategic design and three-dimensional analysis of antiviral drug combinations. Antimicrob. Agents Chemother. 37:540–545.
12. Prichard MN, Shipman C, Jr. 1990. A three-dimensional model to analyze drug-drug interactions. Antiviral Res. 14:181–205.
13. Chou TC, Talalay P. 1984. Quantitative analysis of dose-effect relationships: the combined effects of multiple drugs or enzyme inhibitors. Adv. Enzyme Regul. 22:27–55.
14. Pirrone V, Thakkar N, Jacobson JM, Wigdahl B, Krebs FC. 2011. Combinatorial approaches to the prevention and treatment of HIV-1 infection. Antimicrob. Agents Chemother. 55:1831–1842.
15. Chang CN, Skalski V, Zhou JH, Cheng YC. 1992. Biochemical pharmacology of (+)- and (−)-2′,3′-dideoxy-3′-thiacytidine as anti-hepatitis B virus agents. J. Biol. Chem. 267:22414–22420.
16. Sabini E, Hazra S, Konrad M, Lavie A. 2007. Nonenantioselectivity property of human deoxycytidine kinase explained by structures of the enzyme in complex with L- and D-nucleosides. J. Med. Chem. 50:3004–3014.
17. Hachiya A, Kodama EN, Schuckmann MM, Kirby KA, Michailidis E, Sakagami Y, Oka S, Singh K, Sarafianos SG. 2011. K70Q adds high-level tenofovir resistance to "Q151M complex" HIV reverse transcriptase through the enhanced discrimination mechanism. PLoS One 6:e16242. doi:10.1371/journal.pone.0016242.
18. Kirby KA, Marchand B, Ong YT, Ndongwe TP, Hachiya A, Michailidis E, Leslie MD, Sietsema DV, Fetterly TL, Dorst CA, Singh K, Wang Z, Parniak MA, Sarafianos SG. 2012. Structural and inhibition studies of the RNase H function of xenotropic murine leukemia virus-related virus reverse transcriptase. Antimicrob. Agents Chemother. 56:2048–2061.
19. Nakata H, Amano M, Koh Y, Kodama E, Yang G, Bailey CM, Kohgo S, Hayakawa H, Matsuoka M, Anderson KS, Cheng YC, Mitsuya H. 2007. Activity against human immunodeficiency virus type 1, intracellular metabolism, and effects on human DNA polymerases of 4′-ethynyl-2-fluoro-2′-deoxyadenosine. Antimicrob. Agents Chemother. 51:2701–2708.
20. Abdool Karim Q, Abdool Karim SS, Frohlich JA, Grobler AC, Baxter C, Mansoor LE, Kharsany AB, Sibeko S, Mlisana KP, Omar Z, Gengiah TN, Maarschalk S, Arulappan N, Mlotshwa M, Morris L, Taylor D. 2010. Effectiveness and safety of tenofovir gel, an antiretroviral microbicide, for the prevention of HIV infection in women. Science 329:1168–1174.
21. Grant RM, Lama JR, Anderson PL, McMahan V, Liu AY, Vargas L, Goicochea P, Casapia M, Guanira-Carranza JV, Ramirez-Cardich ME, Montoya-Herrera O, Fernandez T, Veloso VG, Buchbinder SP, Chariyalertsak S, Schechter M, Bekker LG, Mayer KH, Kallas EG, Amico KR, Mulligan K, Bushman LR, Hance RJ, Ganoza C, Defechereux P, Postle B, Wang F, McConnell JJ, Zheng JH, Lee J, Rooney JF, Jaffe HS, Martinez AI, Burns DN, Glidden DV. 2010. Preexposure chemoprophylaxis for HIV prevention in men who have sex with men. N. Engl. J. Med. 363:2587–2599.
22. Richman D, Rosenthal AS, Skoog M, Eckner RJ, Chou TC, Sabo JP, Merluzzi VJ. 1991. BI-RG-587 is active against zidovudine-resistant human immunodeficiency virus type 1 and synergistic with zidovudine. Antimicrob. Agents Chemother. 35:305–308.
23. Brennan TM, Taylor DL, Bridges CG, Leyda JP, Tyms AS. 1995. The inhibition of human immunodeficiency virus type 1 in vitro by a non-nucleoside reverse transcriptase inhibitor MKC-442, alone and in combination with other anti-HIV compounds. Antiviral Res. 26:173–187.
24. King RW, Klabe RM, Reid CD, Erickson-Viitanen SK. 2002. Potency of nonnucleoside reverse transcriptase inhibitors (NNRTIs) used in

combination with other human immunodeficiency virus NNRTIs, NRTIs, or protease inhibitors. Antimicrob. Agents Chemother. 46: 1640–1646.
25. **Maga G, Hubscher U, Pregnolato M, Ubiali D, Gosselin G, Spadari S.** 2001. Potentiation of inhibition of wild-type and mutant human immunodeficiency virus type 1 reverse transcriptases by combinations of nonnucleoside inhibitors and D- and L-(beta)-dideoxynucleoside triphosphate analogs. Antimicrob. Agents Chemother. 45:1192–1200.
26. **Borkow G, Arion D, Wainberg MA, Parniak MA.** 1999. The thiocarboxanilide nonnucleoside inhibitor UC781 restores antiviral activity of 3′-azido-3′-deoxythymidine (AZT) against AZT-resistant human immunodeficiency virus type 1. Antimicrob. Agents Chemother. 43:259–263.
27. **Odriozola L, Cruchaga C, Andreola M, Dolle V, Nguyen CH, Tarrago-Litvak L, Perez-Mediavilla A, Martinez-Irujo JJ.** 2003. Non-nucleoside inhibitors of HIV-1 reverse transcriptase inhibit phosphorolysis and resensitize the 3′-azido-3′-deoxythymidine (AZT)-resistant polymerase to AZT-5′-triphosphate. J. Biol. Chem. 278:42710–42716.
28. **Cruchaga C, Odriozola L, Andreola M, Tarrago-Litvak L, Martinez-Irujo JJ.** 2005. Inhibition of phosphorolysis catalyzed by HIV-1 reverse transcriptase is responsible for the synergy found in combinations of 3′-azido-3′-deoxythymidine with nonnucleoside inhibitors. Biochemistry 44:3535–3546.
29. **Basavapathruni A, Bailey CM, Anderson KS.** 2004. Defining a molecular mechanism of synergy between nucleoside and nonnucleoside AIDS drugs. J. Biol. Chem. 279:6221–6224.
30. **Radzio J, Sluis-Cremer N.** 2008. Efavirenz accelerates HIV-1 reverse transcriptase ribonuclease H cleavage, leading to diminished zidovudine excision. Mol. Pharmacol. 73:601–606.
31. **Shaw-Reid CA, Feuston B, Munshi V, Getty K, Krueger J, Hazuda DJ, Parniak MA, Miller MD, Lewis D.** 2005. Dissecting the effects of DNA polymerase and ribonuclease H inhibitor combinations on HIV-1 reverse-transcriptase activities. Biochemistry 44:1595–1606.
32. **Parikh UM, Koontz DL, Chu CK, Schinazi RF, Mellors JW.** 2005. In vitro activity of structurally diverse nucleoside analogs against human immunodeficiency virus type 1 with the K65R mutation in reverse transcriptase. Antimicrob. Agents Chemother. 49:1139–1144.

Free Radical Biology and Medicine 65 (2013) 778–788

Contents lists available at ScienceDirect

Free Radical Biology and Medicine

journal homepage: www.elsevier.com/locate/freeradbiomed

Original Contribution

Comparative analysis of ER stress response into HIV protease inhibitors: Lopinavir but not darunavir induces potent ER stress response via ROS/JNK pathway

Manabu Taura [a], Ryusho Kariya [a], Eriko Kudo [a], Hiroki Goto [a], Takao Iwawaki [b], Masayuki Amano [c], Mary Ann Suico [d], Hirofumi Kai [d], Hiroaki Mitsuya [c], Seiji Okada [a,*]

[a] Division of Hematopoiesis, Center for AIDS Research, Kumamoto University, 2-2-1 Honjo, Kumamoto, 860-0811, Japan
[b] Iwawaki Laboratory, Advanced Scientific Research Leaders Development Unit, Gunma University, Maebashi 371-8511, Japan
[c] Department of Infectious Diseases and Hematology, Kumamoto University Graduate School of Medical Sciences, Kumamoto University, Kumamoto 860-8556, Japan
[d] Department of Molecular Medicine, Graduate School of Pharmaceutical Sciences, Kumamoto University, Kumamoto 862-0973, Japan

ARTICLE INFO

Article history:
Received 18 April 2013
Received in revised form
11 July 2013
Accepted 9 August 2013
Available online 20 August 2013

Keywords:
AIDS
HIV protease inhibitor
ER stress
CHOP
JNK
ROS

ABSTRACT

HIV protease inhibitor (PI)-induced ER stress has been associated with adverse effects. Although it is a serious clinical problem for HIV/AIDS patients, comparative analyses of ER stress induction by clinically used PIs have rarely been done. Especially, there is no report on the differential ER stress response between lopinavir (LPV) and darunavir (DRV), although these PIs are the most clinically used PIs. We show here that LPV induces the most potent CHOP expression, ER stress marker, among the 9 Food and Drug Administration (FDA)-approved PIs in human peripheral blood mononuclear cells, several human epithelial cells, and mouse embryonic fibroblasts. LPV induced the most potent ROS production and JNK activation in 9 PIs. A comparison among the most clinically used PIs, ritonavir (RTV), LPV, and DRV, revealed that LPV potently and RTV moderately but not DRV induced ER stress via ROS-dependent JNK activation rather than proteasome inhibition. Finally, we analyzed ER stress induction in tissues of mice intraperitoneally injected with RTV, LPV, and DRV. RTV and LPV but not DRV showed ER stress induction in several mice tissues. In conclusion, we first identify LPV as the most potent ER stress inducing PI among 9 FDA-approved PIs in human cells, and although clinical verification is necessary, we show here that DRV has the advantage of less ROS and ER stress induction potential compared with LPV *in vitro* and *in vivo*.

Introduction

The combination antiretroviral therapy (cART) effectively improves HIV/AIDS patients' life prognosis [1]. The HIV-1 protease inhibitor (PI) is a component of this combination therapy based on its suppressive effect on HIV-1 protease and viral maturation to block viral proliferation [2]. Various PIs have been developed in recent years. Ritonavir (RTV)-boosted lopinavir (LPV) and darunavir (DRV) are the most clinically used PIs for cART because these drugs have high binding affinity to HIV-1 protease and are highly active to drug-resistant HIV-1 [3–5]. But despite rigorous drug development PIs do not completely cure HIV/AIDS, and HIV/AIDS patients are required to maintain long-term PI treatment, which causes serious side effects such as hyperlipidemia, diabetes, diarrhea, and atherosclerosis [6].

ER stress is a common molecular mechanisms for PI-induced side effects. Several PIs disrupt lipid metabolism in hepatocytes [7], induce apoptosis in pancreatic β cells to inhibit insulin secretion [8], activate the expression of inflammatory cytokines in macrophage [9], and disrupt the barrier integrity in intestinal epithelial cells [10] via ER stress induction as a common molecular mechanism. Although ER stress is thought to be important for the induction of several side effects by PIs, exhaustive comparison of clinically used PIs in terms of their potential to induce ER stress has not been done. Additionally, there is no report comparing the ER stress-inducing effects of LPV and DRV despite some clinical reports indicating the less adverse effects of DRV compared to those of LPV [11–15].

The accumulation of unfolded proteins, calcium disruption, and ROS production are well known triggers of ER stress [16]. Physiologically, ER stress correlates to several diseases such as diabetes,

Abbreviations: APV, Amprenavir; ARE, antioxidant response; ATV, Atazanavir; cART, Combination antiretroviral therapy; DRV, Darunavir; FDA, Food and Drug Administration; IDV, Indinavir; LDH, lactate dehydrogenase; LPV, Lopinavir; NAC, N-acetyl-L-cysteine; NFV, Nelfinavir; PBMC, Peripheral blood mononuclear cells; PI, Protease inhibitor; PRI, Propidium iodide; RTV, Ritonavir; SQV, Saquinavir; TPV, Tiprenavir

* Corresponding author. Fax: +81 96 373 6523.
E-mail addresses: okadas@kumamoto-u.ac.jp, okada-sj@umin.ac.jp (S. Okada).

0891-5849/$ - see front matter © 2013 Elsevier Inc. All rights reserved.
http://dx.doi.org/10.1016/j.freeradbiomed.2013.08.161